© 2017. Published by The Company of Biologists Ltd | Journal of Cell Science (2017) 130, 2292-2305 doi:10.1242/jcs.196659

RESEARCH ARTICLE

TRPC1 is a differential regulator of hypoxia-mediated events and Akt signalling in PTEN-deficient breast cancer cells

Iman Azimi[1,2,3], Michael J. G. Milevskiy[4], Elke Kaemmerer[1,2,3], Dane Turner[1], Kunsala T. D. S. Yapa[1], Melissa A. Brown[4], Erik W. Thompson[3,5,6], Sarah J. Roberts-Thomson[1] and Gregory R. Monteith[1,2,3,*]

ABSTRACT

Hypoxia is a feature of the tumour microenvironment that promotes invasiveness, resistance to chemotherapeutics and cell survival. Our studies identify the transient receptor potential canonical-1 (TRPC1) ion channel as a key component of responses to hypoxia in breast cancer cells. This regulation includes control of specific epithelial to mesenchymal transition (EMT) events and hypoxia-mediated activation of signalling pathways such as activation of the EGFR, STAT3 and the autophagy marker LC3B, through hypoxia-inducible factor-1α (HIF1α)-dependent and -independent mechanisms. TRPC1 regulated HIF1α levels in PTEN-deficient MDA-MB-468 and HCC1569 breast cancer cell lines. This regulation arises from effects on the constitutive translation of HIF1α under normoxic conditions via an Akt-dependent pathway. In further support of the role of TRPC1 in EMT, its expression is closely associated with EMT- and metastasis-related genes in breast tumours, and is enhanced in basal B breast cancer cell lines. TRPC1 expression is also significantly prognostic for basal breast cancers, particularly those classified as lymph node positive. The defined roles of TRPC1 identified here could be therapeutically exploited for the control of oncogenic pathways in breast cancer cells.

KEY WORDS: Breast cancer, Ca^{2+}, Hypoxia, Akt, PTEN, TRPC1, Signal transduction

INTRODUCTION

The microenvironment of breast tumours is dynamic and can be a key factor in contributing to breast cancer progression (Bissell and Hines, 2011). One essential feature of the breast tumour microenvironment is hypoxia (Semenza, 2016). Hypoxia in breast tumours is a trigger for angiogenesis and other processes important in metastasis, and in the preparation of the metastatic niche (Semenza, 2013). Hypoxia is also crucial for the promotion of breast cancer cells to a more invasive phenotype via epithelial to mesenchymal transition (EMT) (Cooke et al., 2012; Lester et al., 2007).

[1]The School of Pharmacy, The University of Queensland, Brisbane, Queensland, 4102, Australia. [2]Mater Research Institute, The University of Queensland, Brisbane, Queensland, 4101, Australia. [3]Translational Research Institute, Brisbane, Queensland, 4102, Australia. [4]The School of Chemistry and Molecular Biosciences, The University of Queensland, Brisbane, Queensland, 4072, Australia. [5]Institute of Health and Biomedical Innovation and School of Biomedical Sciences, Queensland University of Technology, Brisbane, Queensland, 4059, Australia. [6]University of Melbourne, Department of Surgery, St. Vincent's Hospital, Melbourne, Victoria, 3065, Australia.

*Author for correspondence (gregm@uq.edu.au)

I.A., 0000-0001-9477-9999; K.T.D.S.Y., 0000-0003-0661-0881; G.R.M., 0000-0002-4345-530X

Received 22 August 2016; Accepted 23 May 2017

EMT in breast cancer cells is associated with a remodelling of cellular adhesion through the loss of epithelial markers such as E-cadherin, increased levels of specific transcription factors such as Snail, Zeb and Twist family proteins, and the expression of mesenchymal markers such as the intermediate filament protein vimentin (Tomaskovic-Crook et al., 2009; Ye and Weinberg, 2015). EMT is also associated with the acquisition of resistance to many antineoplastic agents and increased invasiveness (Ye and Weinberg, 2015). We recently identified the Ca^{2+} signal as a regulator of the induction of the EMT marker vimentin by epidermal growth factor (EGF) (Davis et al., 2013). Hence, components of Ca^{2+} signalling in breast cancer cells may represent opportunities to selectively exploit and control specific metastatic and resistance pathways associated with EMT.

Ca^{2+}-permeable ion channels represent important and selective regulators of intracellular Ca^{2+} homeostasis and responses to external stimuli, and are encoded by over 40 genes. Transient receptor potential (TRP) ion channels (Wu et al., 2010) have clear physiological and pathological roles, and often act as sensors of changing environmental cues. TRPV1 is a heat-responsive ion channel, TRPM8 senses cold, and TRPM2 is sensitive to oxidative stress (Wu et al., 2010) and is fundamental in signalling cascades responsible for acetaminophen (paracetamol)-induced liver damage (Kheradpezhouh et al., 2014). TRPC5 is important in semaphorin 3A-induced neuronal growth cone collapse (Kaczmarek et al., 2012) and fear-related behaviour (Riccio et al., 2009), and is also associated with the acquisition of multidrug resistance in breast cancer cells (Ma et al., 2012, 2014). TRPC1 was the first TRP ion channel identified in mammals (Wu et al., 2010) and it is expressed in a variety of cell types (Cheng et al., 2013; Nilius and Szallasi, 2014); however, a detailed understanding of its role(s) in many contexts remains unclear and controversial. TRPC1 has also been described as contributing to store-operated Ca^{2+} entry, often in association with the canonical store-operated Ca^{2+} channel component Orai1 and the Ca^{2+} store sensor STIM1 (Cheng et al., 2013).

TRPC1 is associated with pathophysiological processes in hypoxia in smooth muscle cells of the pulmonary system, being important in pulmonary vascular remodelling associated with chronic hypoxia (Malczyk et al., 2013) and hypoxia-induced enhancement of vascular tone (Xia et al., 2014). Chronic hypoxia is also an inducer of TRPC1 expression in pulmonary arterial smooth muscle cells via hypoxia-inducible factor 1α (HIF1α) (Wang et al., 2006). Despite the link between hypoxia and TRPC1 in the vascular system, no studies have explored the role of TRPC1 in the response to hypoxia in breast cancer cells. We have assessed the potential role of TRPCs in hypoxia-induced EMT in breast cancer cells and show that a specific remodelling of TRPC1 expression is a feature of hypoxia-associated EMT in breast cancer cells via HIF1α. We also define TRPC1 as a regulator of specific hypoxia-induced changes in

Journal of Cell Science

Journal of Cell Science (2017) 130, 2292-2305 doi:10.1242/jcs.196659

EMT marker induction. Unexpectedly, this regulation is through both HIF1α-dependent and -independent mechanisms and involves the differential regulation of specific cellular signalling pathways.

RESULTS

TRPC1 expression is increased during hypoxia and is required for hypoxic induction of Snail and Claudin-4

We assessed the mRNA expression pattern of TRPC family genes in MDA-MB-468 breast cancer cells, with the exception of *TRPC2* (a pseudogene in humans; Yildirim and Birnbaumer, 2007), in both hypoxic and normoxic conditions. *TRPC4*, *-5*, *-6* and *-7* mRNA was not detectable in either hypoxic or normoxic samples (Fig. 1A). While *TRPC3* mRNA levels were not significantly changed upon hypoxia, *TRPC1* mRNA levels were significantly increased (Fig. 1A,Bi). Hypoxia-induced *TRPC1* upregulation was also observed in MDA-MB-231 and HCC1569 breast cancer cells (Fig. S1). *TRPC1* mRNA upregulation in MDA-MB-468 cells was specific to hypoxia, as *TRPC1* mRNA levels were modestly downregulated upon addition of EGF, another EMT inducer (Fig. 1Bii). Hypoxia-induced upregulation of *TRPC1* was dependent on HIF1α, as siRNA-mediated silencing of *HIF1A* (Fig. 1Ci) attenuated hypoxia-induced *TRPC1* mRNA upregulation (Fig. 1Cii). Assessment of potential HIF binding sites in the promoter region of *TRPC1* identified binding motifs for HIF1α and HIF1β (Fig. S2). However, only the silencing of *HIF1A* reduced hypoxia-mediated induction of *TRPC1* mRNA levels (Fig. 1Cii); siRNA against *HIF1B* or *HIF2A* had no effect on the increase in *TRPC1* expression (Fig. S3). Analysis of the gene expression profile of *TRPC1* in human breast cancer cell lines, revealed a significant upregulation of *TRPC1* in Basal B cell lines (which exhibit enhanced mesenchymal-like features; Blick et al., 2010; Neve et al., 2006) compared with other subgroups (Fig. 1D).

To determine whether TRPC1 is involved in the induction of hypoxia-induced EMT, we assessed the effect of its siRNA-mediated silencing on EMT markers. Hypoxia (24 h) resulted in significant upregulation of the mesenchymal markers vimentin, Snail (also known as SNAI1), Twist (TWIST1) and N-cadherin (CDH2), and downregulation of the epithelial marker claudin-4 (CLDN4) (Fig. 1F). Silencing of TRPC1 (Fig. 1E) under hypoxic conditions significantly attenuated the induction of the EMT transcription factor Snail and partially prevented the reduction of the epithelial marker claudin-4 (24 h); however, induction of the other EMT markers by hypoxia was independent of TRPC1 (Fig. 1F). TRPC1 is therefore the first identified ion channel regulator of the EMT transcription factor Snail and epithelial marker claudin-4. This regulation appears to be hypoxia specific as silencing of TRPC1 did not have any significant effect on the basal levels of Snail and claudin-4 in normoxia (Fig. S4). The differential regulation of hypoxia-mediated events was further explored through assessment of cellular signalling pathways activated by hypoxia in breast cancer cells.

TRPC1 is a regulator of hypoxia-induced EGFR and STAT3 activation

EGFR and STAT3 signalling are two key hypoxia-associated signalling pathways (Selvendiran et al., 2009; Pawlus et al., 2014; Peng et al., 2006) that also have important roles in EMT induced by hypoxia (Cui et al., 2016; Misra et al., 2012) and EGF (Lo et al., 2007), although their potential regulation by TRPC1 is unknown. We assessed EGFR at Y1173 (an important site of EGFR autophosphorylation; Kondratov et al., 2010) and STAT3 phosphorylation at Y705 in MDA-MB-468 cells under hypoxic conditions for 6, 24 and 48 h. Phosphorylation of EGFR was significantly enhanced after 24 and 48 h of hypoxia, with no significant concomitant change in total EGFR protein (Fig. 2A). Likewise, total STAT3 protein levels were not altered by hypoxia, but phosphorylation of STAT3 was significantly increased at 24 h (Fig. 2A). Silencing of *TRPC1* with siRNA significantly reduced hypoxia-induced EGFR and STAT3 phosphorylation, with no change in total EGFR or STAT3 levels, respectively (Fig. 2B,C). Given the upregulation of TRPC1 with hypoxia but not EGF (Fig. 1B), the selective role of TRPC1 in hypoxia was explored by silencing *TRPC1* and assessing EGFR and STAT3 phosphorylation induced by EGF. *TRPC1* silencing did not alter EGF-induced phosphorylation of EGFR (Fig. 2D) or inhibit STAT3 phosphorylation (Fig. 2E); instead, augmentation of STAT3 phosphorylation was evident (Fig. 2E). These findings provide further evidence for the selectivity of TRPC1 in hypoxia and identify a role for TRPC1 in hypoxia-induced transactivation of EGFR.

Regulation of non-stimulated and store-operated Ca^{2+}-entry pathways by TRPC1 after hypoxia

TRPC1 has been implicated in store-operated Ca^{2+} entry in some cell types (Cheng et al., 2013). Under normoxic conditions in MDA-MB-468 breast cancer cells, TRPC1 is a regulator of non-stimulated (constitutive) Ca^{2+} influx but not of store-operated Ca^{2+} entry (Davis et al., 2012). To assess whether hypoxia alters the nature of the contribution of TRPC1 to Ca^{2+} influx, we assessed the effects of *TRPC1* silencing on non-stimulated (constitutive) Ca^{2+} influx and store-operated Ca^{2+} entry after hypoxia (Fig. 3). Silencing of *TRPC1* had no effect on the cytosolic free Ca^{2+} ($[Ca^{2+}]_{CYT}$) increases associated with store depletion induced by the sarco/endoplasmic reticulum Ca^{2+} ATPase inhibitor cyclopiazonic acid (CPA) (Fig. 3A,B, peak 1). However, *TRPC1* silencing significantly augmented store-operated Ca^{2+} influx (Fig. 3A,B, peak 2) and reduced non-stimulated Ca^{2+} influx compared with the non-targeting control (Fig. 3A,B). Hence, hypoxia (24 h) was not associated with a change in the nature of the contribution of TRPC1 to basal Ca^{2+} influx or store-operated Ca^{2+} entry, as the effects were identical to those seen with normoxia (Davis et al., 2012).

TRPC1 regulates HIF1α levels and Akt activation in MDA-MB-468 breast cancer cells

As TRPC1 modified specific EMT markers and cellular signalling cascades induced by hypoxia, we sought to determine whether TRPC1 was involved in the early induction of the hypoxic transcriptional regulator HIF1α. Pronounced accumulation of HIF1α protein was evident at 6 h, and this early induction was significantly inhibited by silencing of *TRPC1* (Fig. 4A and Fig. S6A). We assessed whether this regulation was solely through the reduced ability of cells to sense reduced O_2 levels by silencing *TRPC1* and examining basal protein and mRNA levels of HIF1α under normoxic conditions. Consistent with its status as a PTEN-deficient breast cancer cell line (Li et al., 1997; Zundel et al., 2000), MDA-MB-468 breast cancer cells exhibited some basal expression of HIF1α protein, which was almost completely abolished upon *TRPC1* silencing (Fig. 4B), and this effect was not mediated through a decrease in *HIF1A* mRNA levels (Fig. 4C). Hence, the effect of TRPC1 on HIF1α protein did not occur via transcriptional modulation but rather via effects on HIF1α translational and/or degradation.

Hypoxia-induced HIF1α protein stabilisation is predominantly via inhibition of proteasome-mediated degradation as a result of low levels of O_2 (Salceda and Caro, 1997). To assess if TRPC1 regulation of HIF1α protein was through this O_2-dependent

Journal of Cell Science

Journal of Cell Science (2017) 130, 2292-2305 doi:10.1242/jcs.196659

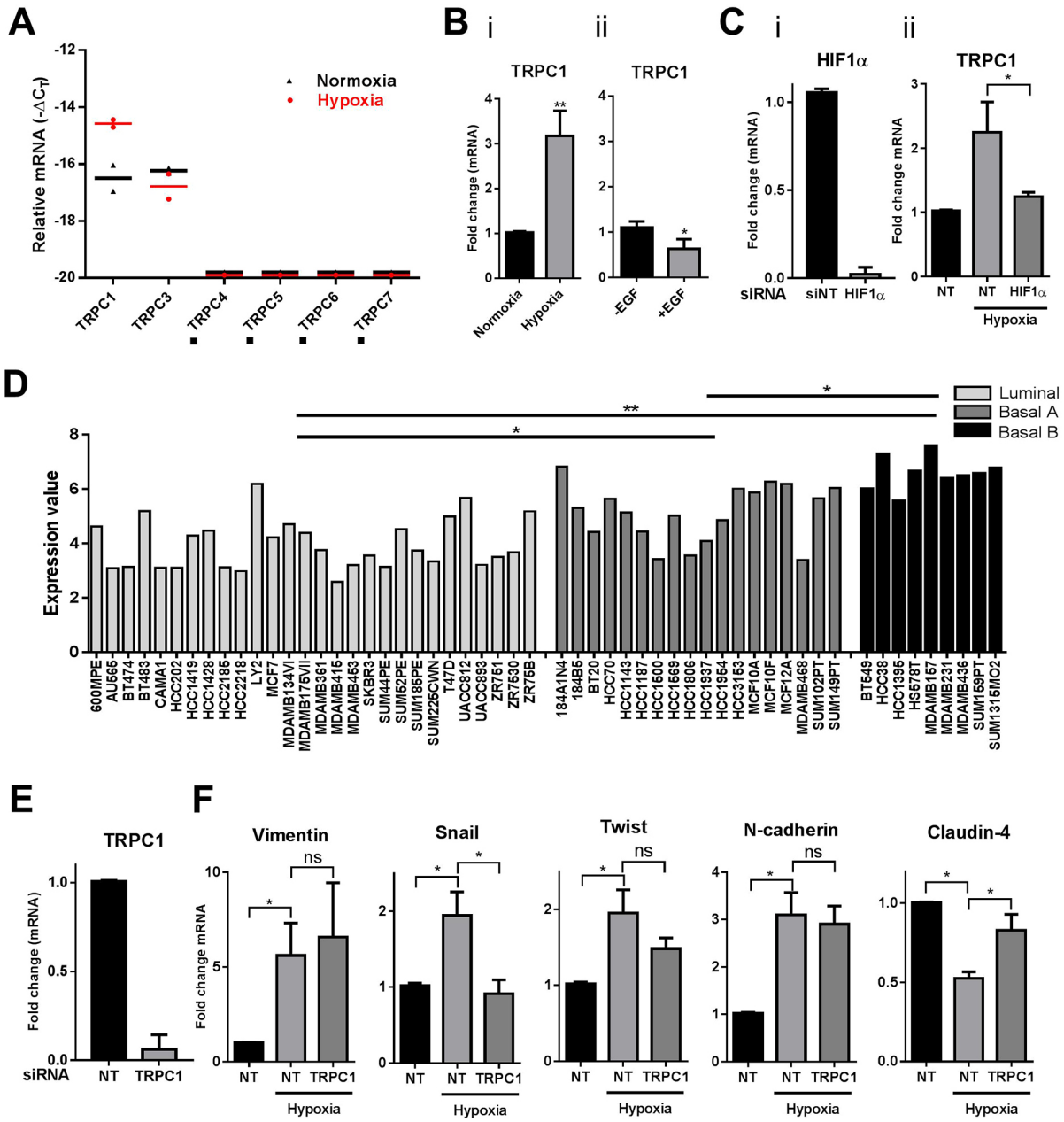

Fig. 1. *TRPC1* expression is upregulated by hypoxia via HIF1α and its silencing attenuates hypoxia-induced changes in Snail and claudin-4. (A) Transcriptional profile of TRPC isoforms [relative mRNA ($-\Delta C_T$)] showed selective upregulation of *TRPC1* with hypoxia (24 h) [■ denotes a target below the limit of detection (C_T >35)]. (B) *TRPC1* induction in MDA-MB-468 cells 24 h after hypoxia (i) or 50 ng/ml EGF (ii). **P*<0.05, ***P*<0.01 compared with control (unpaired *t*-test), *n*=3, mean±s.d. (C) siRNA-mediated silencing of *HIF1A* relative to non-targeting control (NT) (i) and its effect on hypoxia-induced *TRPC1* mRNA upregulation (24 h hypoxia, ii). **P*<0.01 (one-way ANOVA, with Bonferroni's multiple comparisons), *n*=3, mean±s.d. (D) TRPC1 assessment in gene expression data of 50 breast cancer cell lines and 5 non-malignant breast cell lines, including three subtypes of luminal, basal A and basal B/mesenchymal. Data are from Array Express (accession no. E-MTAB-181) (Heiser et al., 2012) and are normalised log2-transformed values; **P*<0.001, ***P*<0.0001 (one-way ANOVA, with Tukey's multiple comparisons). (E) Confirmation of *TRPC1* siRNA-mediated silencing. (F) Effect of *TRPC1* silencing on hypoxia-mediated induction of EMT markers in MD-MB-468 cells. **P*<0.01 (one-way ANOVA, with Bonferroni's multiple comparisons), ns, not significant; *n*=3, mean±s.d.

proteolysis mechanism, we treated *TRPC1*-silenced and control cells with the proteasome inhibitor MG132 (Salceda and Caro, 1997). As expected, MG132 treatment increased HIF1α protein levels (Fig. 4D) and siRNA-mediated silencing of *TRPC1* reduced the MG132-induced increases in HIF1α (Fig. 4D). TRPC1 does not, therefore, regulate HIF1α via proteasome-mediated degradation.

Another possible intersection between HIF1α and TRPC1 could be via Akt (AKT1). HIF1α translation is upregulated by Akt (Pore et al., 2006), and Akt activity is enhanced in PTEN-deficient cells (Cantley and Neel, 1999; deGraffenried et al., 2004; Soria et al., 2002), which include MDA-MB-468 cells (Li et al., 1997). We therefore assessed the effects of *TRPC1* silencing on the constitutive activation of Akt and the role of the Akt pathway on HIF1α levels in MDA-MB-468 cells. These studies were performed under normoxic conditions since we showed that TRPC1 could regulate HIF1α levels in the absence of hypoxia (see Fig. 4B). *TRPC1* silencing significantly reduced basal Akt phosphorylation but not total levels of Akt protein (Fig. 4E), whereas basal phosphorylation of both

Journal of Cell Science

Journal of Cell Science (2017) 130, 2292-2305 doi:10.1242/jcs.196659

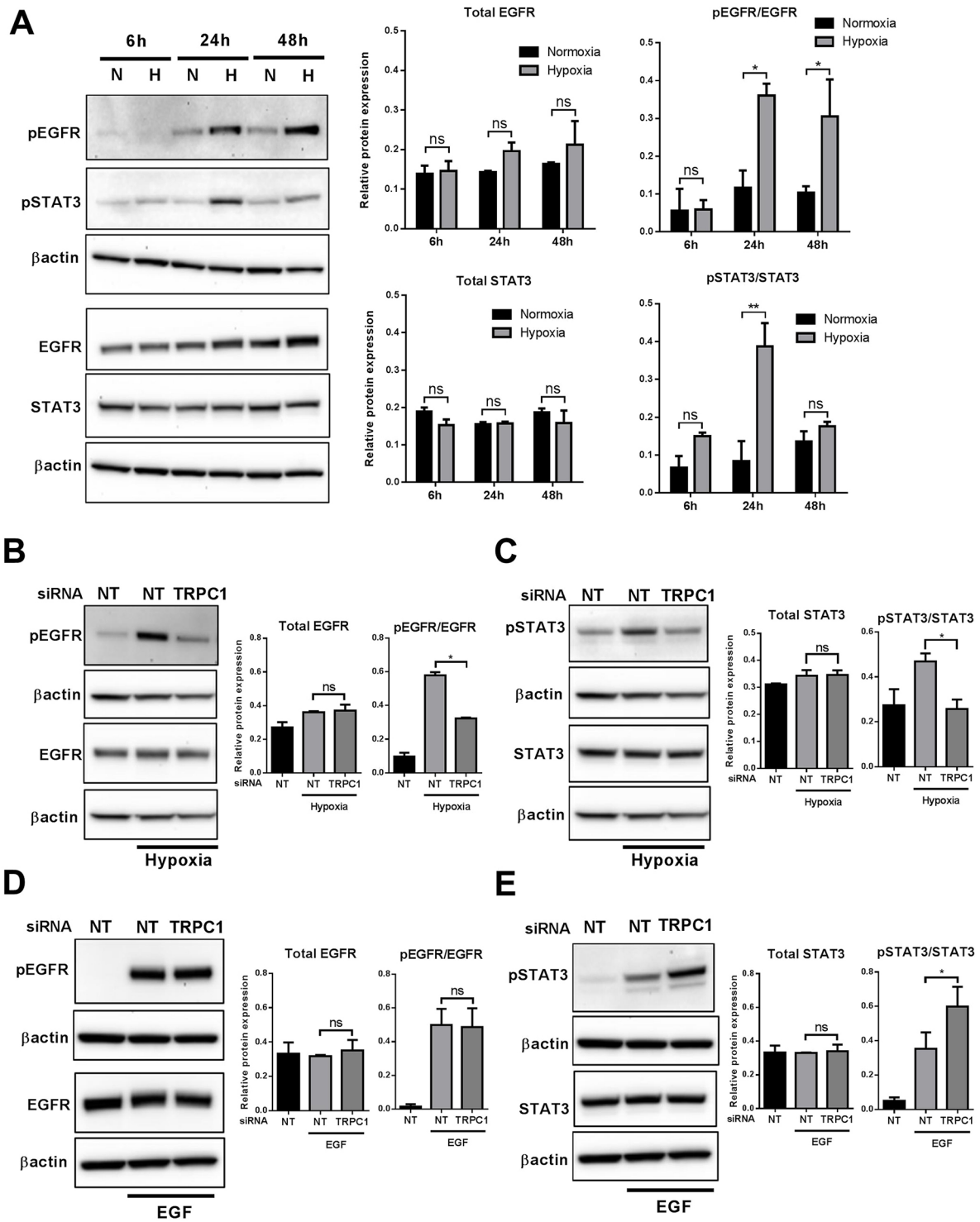

Fig. 2. TRPC1 promotes hypoxia but not EGF-induced EGFR(Y1173) and STAT3(Y705) phosphorylation. (A) MDA-MB-468 breast cancer cells were serum reduced (24 h) and exposed to hypoxia for 6, 24 and 48 h; representative immunoblot and densitometry analysis of total EGFR and STAT3 (normalised to β-actin) and phosphorylated EGFR (Y1173) and STAT3 (Y705) (normalised to β-actin and total EGFR and STAT3). **P*<0.01, ***P*<0.001 (two-way ANOVA, with Bonferroni's multiple comparisons); ns, not significant. (B) Representative immunoblot and densitometry analysis of the effect of *TRPC1* silencing on total EGFR protein and phosphorylation with hypoxia (24 h). **P*<0.001 (one-way ANOVA, with Bonferroni's multiple comparisons). (C) Representative immunoblot and densitometry analysis of the effect of *TRPC1* silencing on total STAT3 protein and phosphorylation with hypoxia (24 h). **P*<0.01 (Bonferroni one-way ANOVA). (D) Representative immunoblot and densitometry analysis of the effect of *TRPC1* silencing on total EGFR protein and phosphorylated levels with EGF (20 min). (E) Representative immunoblot and densitometry analysis of the effect of *TRPC1* silencing on total STAT3 protein and phosphorylation with EGF (20 min). **P*<0.05 (Bonferroni one-way ANOVA). The same membrane was blotted for both STAT3 and EGFR (both total and phosphorylated), and therefore the same β-actin loading controls are used for comparisons in B and C, and D and E, respectively. All densitometry data presented are the mean±s.d. of three independent experiments and normalised to β-actin. Relative protein expression is defined as quantification of fraction of total protein band intensity after normalisation to β-actin loading control.

Journal of Cell Science

Journal of Cell Science (2017) 130, 2292-2305 doi:10.1242/jcs.196659

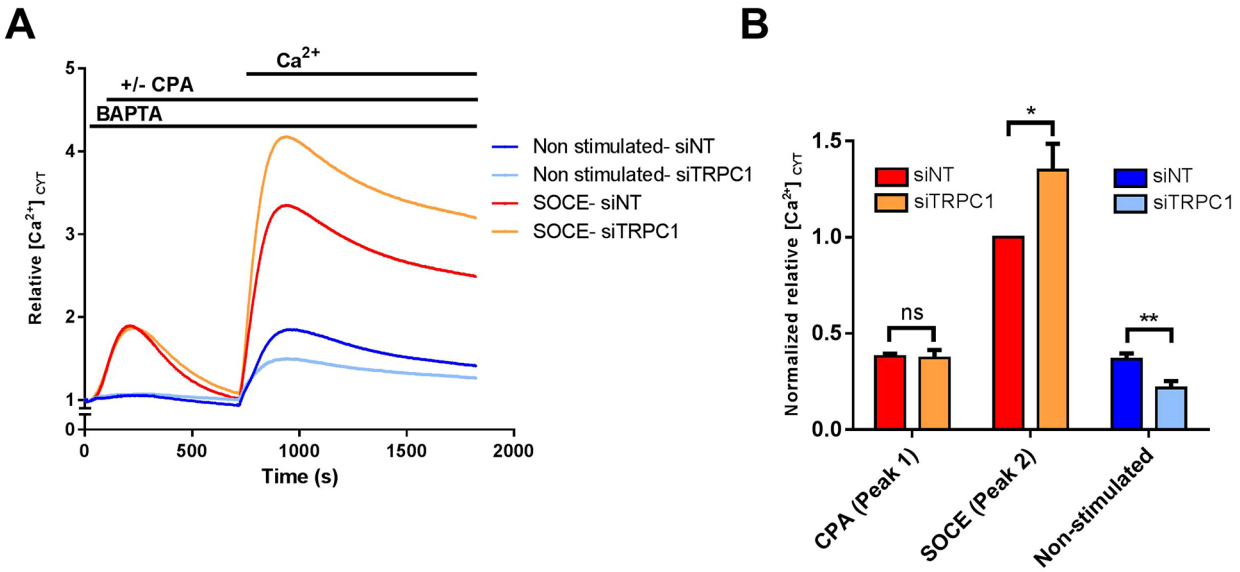

Fig. 3. *TRPC1* silencing attenuates non-stimulated Ca^{2+} influx and augments store-operated Ca^{2+} entry after hypoxia in MDA-MB-468 breast cancer cells. (A) Mean $[Ca^{2+}]_{CYT}$ levels during assessment of non-stimulated Ca^{2+} influx (DMSO control) and store-operated Ca^{2+} entry (SOCE; 10 µM CPA) with or without *TRPC1* siRNA silencing after exposure to hypoxia (24 h). (B) Quantification of relative $[Ca^{2+}]_{CYT}$ (mean±s.d., n=3) normalised to the maximum peak height of the store-operated Ca^{2+} entry of the non-targeting siRNA control. For each group, the siTRPC1 is compared with its non-targeting (NT) control. *P<0.05, **P<0.01 (unpaired t-test).

EGFR and STAT3 were unaffected in normoxia (Fig. 4E), unlike the decrease seen with *TRPC1* silencing and hypoxia-induced EGFR and STAT3 phosphorylation (Fig. 2B,C). MK-2206 2HCl, an Akt-selective inhibitor, concentration-dependently phenocopied the suppression of basal HIF1α levels by *TRPC1* silencing (Fig. 4F), implicating Akt as the conduit between TRPC1 and HIF1α translation. Similarly, in *PTEN*-null HCC1569 breast cancer cells (Chou et al., 2009), *TRPC1* silencing (Fig. 4Gi) significantly reduced both basal Akt phosphorylation (Fig. 4Gii) and basal HIF1α expression (Fig. 4Giii). To confirm this observation, we overexpressed TRPC1 using a commercially available TRPC1 plasmid (Fig. 4Hi) and examined the levels of HIF1α and Akt phosphorylation (Fig. 4Hii). The data show that TRPC1 overexpression is sufficient to induce HIF1α and Akt phosphorylation, and this induction of HIFα is inhibited by Akt inhibition (Fig. 4Hii). These results highlight the important role of TRPC1 in the Akt–HIF1α pathway in PTEN-deficient breast cancer cells, even under normoxic conditions.

HIF1A silencing attenuates hypoxia-mediated changes in *SNAI1* gene expression and non-stimulated Ca^{2+} influx

Since we showed that HIF1α is a TRPC1-sensitive protein in this model, we assessed whether HIF1α is an intermediate between TRPC1 and the induction of EMT markers and cellular signalling cascades induced by hypoxia. To achieve this aim, we silenced *HIF1A* and compared these effects with those observed upon *TRPC1* silencing. Some of the effects of *TRPC1* silencing were independent of HIF1α. Silencing of *HIF1A* phenocopied the effects of *TRPC1* silencing on hypoxia-induced changes in the expression of Snail but not claudin-4 (Fig. 5A). Despite the ability of HIF1α to regulate TRPC1 expression (as shown in Fig. 1C), *HIF1A* silencing had the opposite effect of *TRPC1* silencing on hypoxia-mediated changes in EGFR and STAT3 phosphorylation (Fig. 5B). Although this result may be unexpected, it is not totally surprising given that TRPC1 expression is not reduced to the same degree by silencing of *HIF1A* compared with *TRPC1*. Furthermore, HIF1α as a hypoxic transcriptional regulator, may influence other pathways that may have opposing effects to those of TRPC1 on EGFR and STAT3 activity. However, these results do clearly define effects of TRPC1 that are independent of HIF1α, namely hypoxia-induced changes in claudin-4 expression and EGFR and STAT3 phosphorylation. The differential contribution of HIF1α to the effects of *TRPC1* silencing was also evident when assessing Ca^{2+} homeostatsis. *HIF1A* silencing reduced constitutive Ca^{2+} influx in a similar manner to that seen with silencing of *TRPC1*; however, *HIF1A* siRNA did not promote store-operated Ca^{2+} entry, as was seen upon *TRPC1* siRNA treatment (Fig. 5C). Hence, some of the responses of breast cancer cells to hypoxia are clearly influenced by TRPC1, but the contribution of TRPC1 appears to involve both HIF1α-dependent and -independent mechanisms.

TRPC1 modulates hypoxia-induced changes in the autophagy marker LC3B via regulation of EGFR

In addition to EMT, one other event associated with hypoxia is autophagy. Autophagy is a key hypoxia-induced survival mechanism seen in some cancer cells (Hu et al., 2012), and is Ca^{2+} signalling dependent (Cárdenas et al., 2010; Decuypere et al., 2013; Kondratskyi et al., 2013; Parys et al., 2012). *TRPC1* silencing significantly reduced the protein levels of the hypoxia-induced autophagy marker LC3BII (also known as MAP1LC3BII, where II indicates the lipidated form) (Fig. 6A and Fig. S6B). Silencing of *EGFR* also significantly attenuated hypoxia-induced elevation of LC3BII levels, whereas silencing of either *STAT3* or *HIF1A* had no significant effect (Fig. 6B). These results suggest that hypoxia increases LC3BII levels via a TRPC1 pathway that is dependent on EGFR phosphorylation but is independent of TRPC1-mediated regulation of hypoxia-induced changes in HIF1α levels or STAT3 activity.

TRPC1 is associated with breast cancer molecular subtypes with mesenchymal features and poor prognosis in basal breast cancers

Collectively, the results above implicate *TRPC1* in some of the pathways associated with hypoxia-induced EMT. We assessed

Journal of Cell Science

Journal of Cell Science (2017) 130, 2292-2305 doi:10.1242/jcs.196659

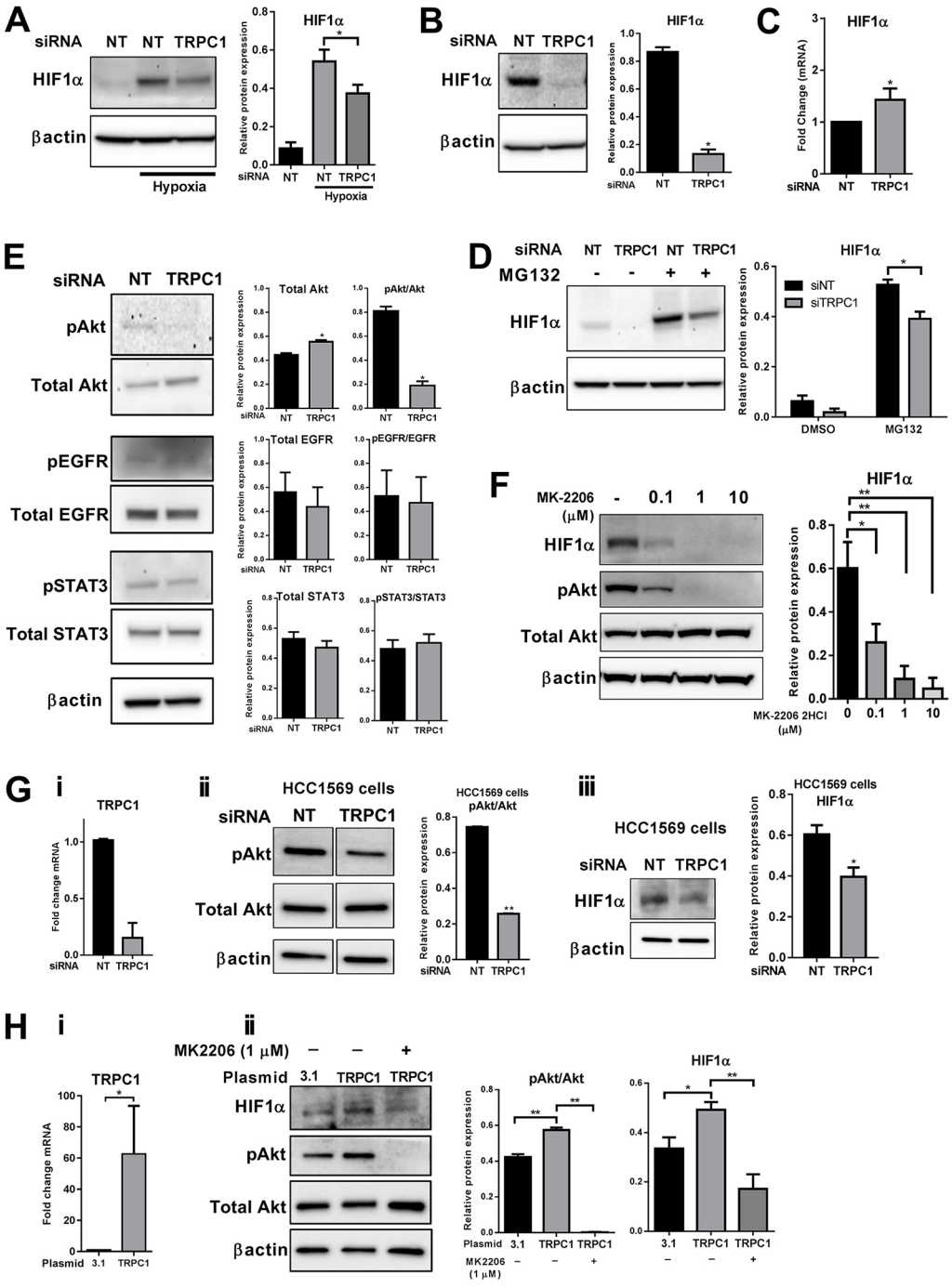

Fig. 4. TRPC1 regulation of HIF1α translation and basal activation of Akt in MDA-MB-468 breast cancer cells in normoxia. (A) Representative immunoblot (left) and quantitative analyses (right) of the effect of *TRPC1* siRNA-mediated silencing on hypoxia-induced (6 h) increases in HIF1α protein compared with NT siRNA in normoxia and hypoxia (n=3, mean±s.d., *P<0.05, one-way ANOVA, with Bonferroni's multiple comparisons). (B) Immunoblot (left) and quantitative analysis (right) of HIF1α protein levels in MDA-MB-468 cells with *TRPC1* and NT siRNA both under normoxic conditions (n=3, mean±s.d., *P<0.001, unpaired t-test). (C) Assessment of the effect of *TRPC1* silencing on *HIF1A* mRNA levels in normoxia (n=3, mean±s.d., *P<0.05, unpaired t-test). (D) Effect of *TRPC1* silencing on MG132 proteasome inhibitor-induced increases in HIF1α protein (n=3, mean±s.d., *P<0.001, two-way ANOVA, with Bonferroni's multiple comparisons). (E) Levels of total and phosphorylated levels of Akt, EGFR and STAT3 in the absence and presence of *TRPC1* siRNA in normoxia (n=3, mean±s.d., *P<0.001, unpaired t-test). (F) Representative immunoblot (left) and quantitative analysis (right) of HIF1α protein levels in MDA-MB-468 cells treated with the Akt inhibitor MK-2206 2HCl for 24 h (n=3, mean±s.d., *P<0.01, **P<0.001, one-way ANOVA, with Bonferroni's multiple comparisons). (G) Confirmation of *TRPC1* silencing (i), and representative immunoblot and quantitative analysis of the basal level of Akt phosphorylation (ii) and HIF1α protein (iii) in HCC1569 cells with *TRPC1* silencing (n=3, mean±s.d., *P<0.01, **P<0.0001 unpaired t-test). All densitometry data are presented as the mean of three independent experiments. The uncropped full blots of Gii are shown in Fig. S5. Relative protein expression is defined as quantification of fraction of total protein band intensity after normalisation to β-actin loading control. (H) TRPC1 plasmid increases *TRPC1* levels compared with PCDNA3.1 control plasmid (3.1) (i; n=3, mean±s.d., *P<0.05, unpaired t-test,). TRPC1 overexpression increases levels of Akt phosphorylation and HIF1α protein in MDA-MB-468 cells and these increases are reduced by the Akt inhibitor MK2206 (1 μM) (ii; n=3, mean±s.d., *P<0.05, **P<0.001, one-way ANOVA, with Bonferroni's multiple comparisons).

Journal of Cell Science

Journal of Cell Science (2017) 130, 2292-2305 doi:10.1242/jcs.196659

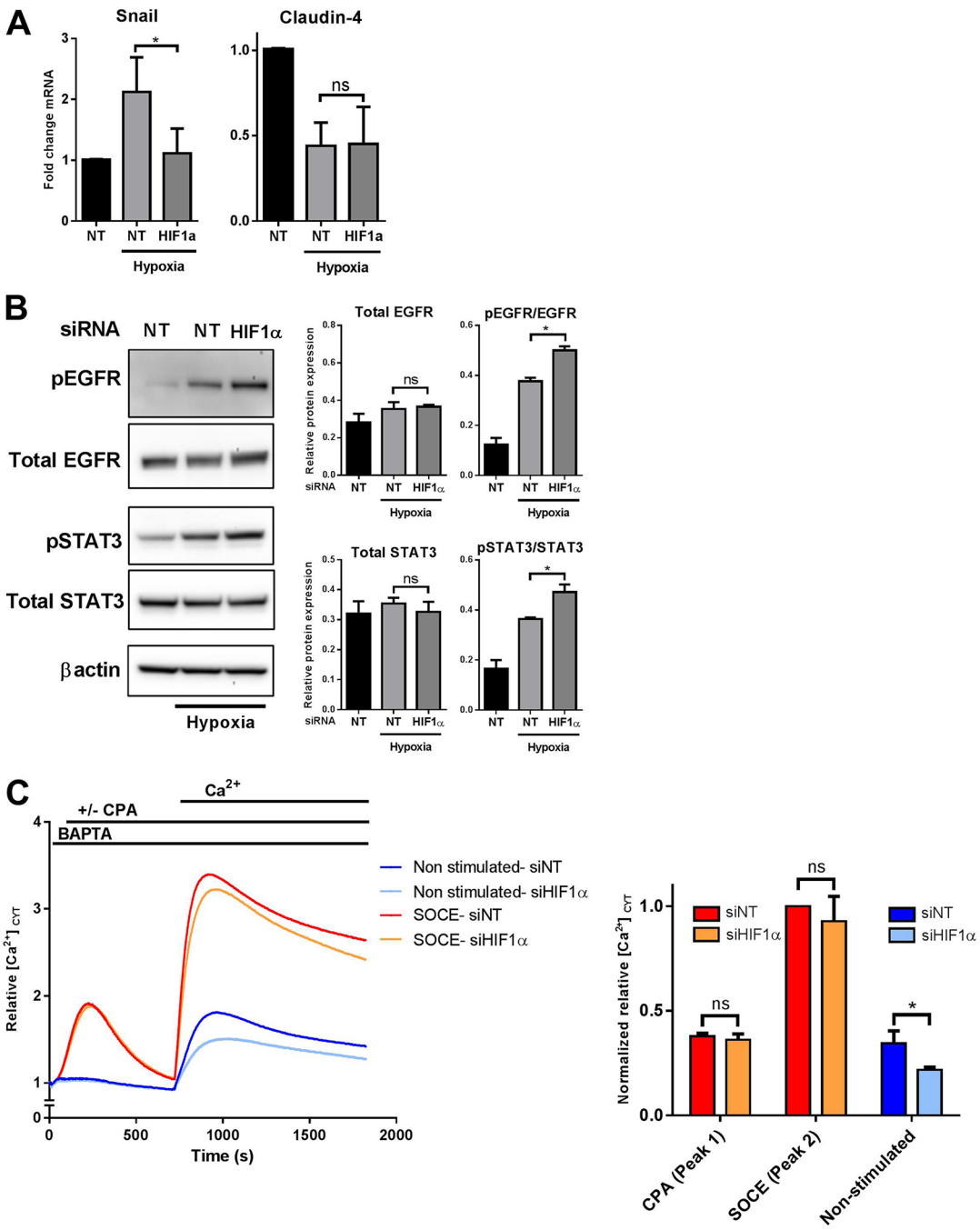

Fig. 5. Assessment of the involvement of HIF1α in hypoxic events regulated by TRPC1. (A) Effect of *HIF1A* siRNA-mediated silencing on the levels of hypoxia (24 h)-mediated upregulation of the mesenchymal marker *SNAI1*, and hypoxia-mediated downregulation of the epithelial marker *Claudin-4* (24 h hypoxia) (n=3, mean±s.d., *P<0.05, one-way ANOVA, with Bonferroni's multiple comparisons). (B) Representative immunoblot (left) and quantitative analyses (right) of the effect of *HIF1A* silencing on the levels of total and phosphorylated EGFR(Y1173) and STAT3(Y705) with 24 h hypoxia. All densitometry data are presented as the mean±s.d. of three independent experiments (*P<0.01, one-way ANOVA, with Bonferroni's multiple comparisons). (C) Mean $[Ca^{2+}]_{CYT}$ levels during assessment of non-stimulated Ca^{2+} influx (DMSO control) and store-operated Ca^{2+} entry (SOCE; 10 µM CPA) with or without *HIF1A* silencing after exposure to hypoxia (24 h) (left), quantification of relative $[Ca^{2+}]_{CYT}$ normalised to the maximum peak height of the store-operated Ca^{2+} entry of the non-targeting siRNA control (right). For each group, the siHIF1α was compared with its non-targeting control. Values are mean±s.d., n=3; *P<0.05, unpaired t-test. Relative protein expression is defined as quantification of the fraction of total protein band intensity after normalisation to β-actin loading control.

whether such an association was also present in clinical breast cancers given that some breast cancer subtypes are more enriched in EMT markers than others. Our assessment of PAM50 breast cancer molecular subtypes (Harrell et al., 2012), showed that the claudin-low (C-Low) subtype (predominantly associated with EMT and stem cell characteristics; Hennessy et al., 2009), had the highest levels of *TRPC1* expression, with significantly higher levels than basal, HER2, luminal A and luminal B breast cancers [Fig. 7A, expression data from The University of North Carolina (UNC) (Harrell et al., 2012); see Materials and methods]. Consistent with this result, assessment of the recently defined triple-negative breast cancer (TNBC) subtypes identified the highest levels of *TRPC1* in

Journal of Cell Science

Journal of Cell Science (2017) 130, 2292-2305 doi:10.1242/jcs.196659

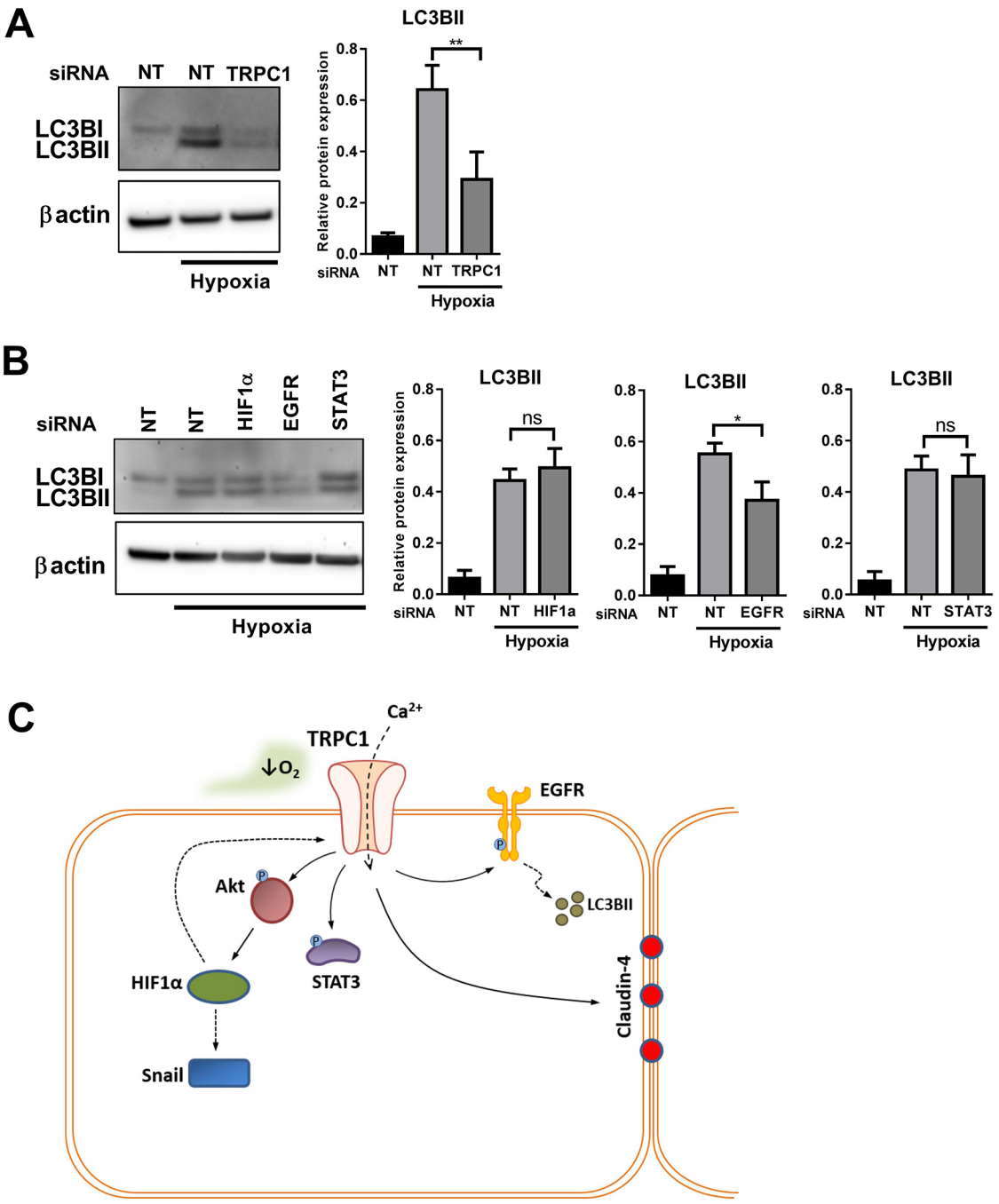

Fig. 6. Regulation of hypoxia-mediated induction of the autophagy marker LC3BII by TRPC1 and EGFR. (A) Assessment of the effect of *TRPC1* silencing on hypoxia (48 h)-mediated upregulation of LC3BII protein. Representative immunoblot (left) and quantitative analyses (right) of the LC3BII band as the active autophagosome membrane-bound form. (B) Representative immunoblot (left) and quantitative analyses (right) of LC3BII levels with siRNA-mediated silencing of *HIF1A*, *EGFR* and *STAT3*. All densitometry data are presented as the mean of three independent experiments (n=3, mean±s.d., *P<0.05, **P<0.01, one-way ANOVA, with Bonferroni's multiple comparisons). Relative protein expression is defined as quantification of fraction of total protein band intensity after normalisation to β-actin loading control. (C) Schematic representation of proposed hypoxia-associated events regulated by TRPC1. TRPC1 regulates HIF-1α protein levels via an Akt-dependent pathway. TRPC1 promotes EMT through upregulation of hypoxia-induced *SNAI1* mRNA expression via a HIF-1α-dependent mechanism and downregulation of *CLDN4*. TRPC1 regulates activation of hypoxia-induced STAT3 and EGFR phosphorylation and hypoxia-induced LC3BII levels via effects on EGFR.

the mesenchymal (MES) subtype, with significantly greater levels than basal-like immune-activated (BLIA) and basal-like immune-suppressed (BLIS) subtypes (Fig. 7B). High levels of TRPC1 are associated with a significantly poorer prognosis in basal breast cancers (Fig. 7C), particularly in basal breast cancers with positive lymph node involvement [Fig. 7D; data sourced from Kaplan–Meier (KM) plotter; Győrffy et al., 2010]. To provide greater insight into those breast cancers with high levels of *TRPC1* expression, the top 100 genes most positively (Table S1) and negatively (Table S2) associated with *TRPC1* in breast cancers were assessed by gene ontology. Genes positively associated with *TRPC1* were significantly enriched for pathways and processes associated with

Journal of Cell Science

Journal of Cell Science (2017) 130, 2292-2305 doi:10.1242/jcs.196659

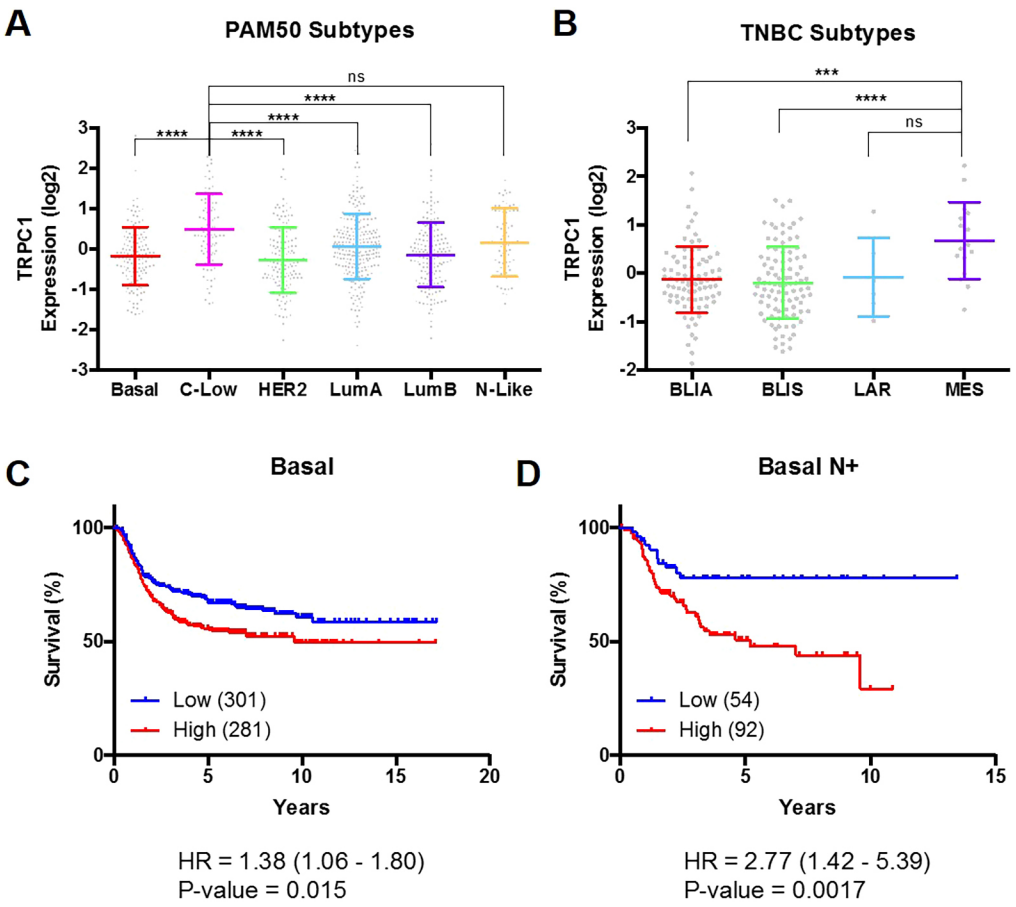

Fig. 7. *TRPC1* expression is enriched in mesenchymal subtypes of breast cancer and stratifies the survival of basal patients with metastatic relapse. (A) Expression of *TRPC1*, log2 transformed, across the five intrinsic subtypes of breast cancer, including the basal and normal-like derived claudin-low (C-Low). (B) Expression of *TRPC1*, log2 transformed, across the four subtypes of triple-negative breast cancer. Expression data sourced from UNC (Harrell et al., 2012). Statistical significance for A and B was obtained via a one-way ANOVA with multiple comparisons corrected via Tukey test. ***P<0.001, ****P<0.0001; ns, not significant. (C,D), Kaplan–Meier curves for the stratification of patient relapse-free survival by TRPC1 expression level in all basal tumours and those that are lymph node-positive (N+). Patient numbers in the high or low expression groups are indicated in brackets, log rank P-values and hazard ratios (HRs) are displayed below each graph; 95% confidence intervals in brackets. Patient survival outcome data sourced from KM-Plotter (see Materials and methods for details).

the mesenchymal phenotype such as those related to wound healing, migration, adhesion and development (Table 1 and Fig. S7). Indeed, these processes are shown to be a consequence of EMT (Tomaskovic-Crook et al., 2009), and the relationship between the positively associated genes with *TRPC1* and these processes further supports the role of TRPC1 in EMT. In contrast, negatively associated genes were associated with features often reduced as a consequence of EMT, such as chromatin assembly, nucleosome organization and M phase (Table 1 and Fig. S8). This analysis of breast cancer subtypes provides further evidence for an association between TRPC1 and some aspects of EMT.

DISCUSSION

As a primary tumour develops, the associated hypoxic environment initiates events such as the induction of a more invasive phenotype through EMT (Azimi and Monteith, 2016; Lester et al., 2007) and cell survival via autophagy (Hu et al., 2012). The studies presented here provide evidence for TRPC1 as a critical regulator of processes induced by hypoxia via HIF1α-dependent and -independent mechanisms. Our studies have also defined a role for TRPC1 in the control of HIF1α expression under normoxic conditions in PTEN-deficient breast cancer cells through an Akt-dependent mechanism.

Initial evidence for a selective role of TRPC1 in hypoxia was the upregulation of TRPC1 with hypoxia-induced EMT but not EGF-induced EMT. Increases in TRPC1 channel expression were sensitive to the silencing of a master regulator of hypoxia responses, *HIF1A* (Weidemann and Johnson, 2008), consistent with the prediction of *TRPC1* as a HIF1α target gene (Ortiz-Barahona et al., 2010). Cellular signalling can selectively control different pathways to EMT induction (Kondratov et al., 2010) and the subsequent array of events that include increased migration, resistance to therapeutic agents and the remodelling of cellular adhesion (Tomaskovic-Crook et al., 2009; Ye and Weinberg, 2015). Our studies provide evidence for TRPC1 as a regulator of hypoxia-mediated EMT pathways associated with changes in claudin-4 and Snail. The observation that TRPC1 is highest in the claudin-low (PAM50) and MES (TNBC) molecular subtypes, provides compelling evidence for an association between TRPC1 and aspects on the EMT pathway, and is consistent with its increased expression in the basal B cell line subgroups, which show enhanced mesenchymal-like features (Neve et al., 2006). The relationship between genes positively correlated with TRPC1 and pathways remodelled in EMT (e.g. wound healing, migration, development, adhesion; Tomaskovic-Crook et al., 2009), further support the placement of TRPC1 as an ion channel regulator of aspects of EMT and therefore potentially metastasis (Semenza, 2013) and/or therapeutic resistance (Fischer et al., 2015). Indeed, we found that elevated TRPC1 levels were associated with poor survival in basal breast cancers, particularly those with lymph node involvement.

TRPC1 is not a master regulator of all changes associated with EMT induced by hypoxia since some EMT markers were insensitive to *TRPC1* silencing. As TRPC1 regulates hypoxia-mediated changes in EMT markers via HIF1α-dependent and -independent mechanisms (Fig. 6C), our work also reflects the specificity of different signals in inducing EMT. The role of TRPC1 in hypoxia-mediated EMT is analogous to the role of the ion channel TRPM7 in the control of EGF-induced protein expression of the EMT marker vimentin, but not Twist and N-cadherin (Davis

Journal of Cell Science

Journal of Cell Science (2017) 130, 2292-2305 doi:10.1242/jcs.196659

Table 1. TRPC1 expression associates positively with mesenchymal ontologies and negatively with proliferation ontologies

Gene ontology term	Reference	Observed	Expected	Fold Enrichment	*P*-value (raw)	*P*-value (adjusted)
Top 100 positively associated genes by expression						
Regulation of wound healing	77	5	0.42	11.87	6.26E−05	2.00E−3
Extracellular matrix organisation	211	9	1.15	7.8	2.18E−06	3.00E−04
Cellular response to growth factor stimulus	277	10	1.51	6.6	2.58E−06	3.00E−04
Ossification	282	9	1.54	5.84	2.27E−05	1.00E−03
Muscle contraction	254	8	1.39	5.76	7.29E−05	2.10E−03
Blood vessel morphogenesis	433	10	2.37	4.22	1.00E−04	2.30E−03
Coagulation	503	11	2.75	4	8.72E−05	2.30E−03
Cell migration	841	17	4.6	3.7	2.30E−06	3.00E−04
Cell adhesion	954	19	5.22	3.64	6.41E−07	2.00E−04
Organ morphogenesis	802	15	4.39	3.42	2.50E−05	1.00E−03
Regulation of cell proliferation	1177	18	6.44	2.8	5.10E−05	1.70E−03
Response to external stimulus	1323	20	7.23	2.76	2.08E−05	9.00E−04
Regulation of cellular component organisation	1214	18	6.64	2.71	7.64E−05	2.20E−03
Anatomical structure formation involved in morphogenesis	1594	22	8.72	2.52	2.99E−05	1.10E−03
Cellular developmental process	2829	30	15.47	1.94	1.00E−04	2.30E−03
Top 100 negatively associated genes by expression						
Chromatin assembly	117	5	0.59	8.45	4.42E−02	4.42E−02
Nucleosome organisation	128	5	0.65	7.72	5.00E−04	4.92E−02
M phase	539	10	2.73	3.67	4.00E−04	4.72E−02

Gene ontology (GO) analysis produced a hierarchical tree of GO terms, the end point term was taken and is summarised in the table. For the full GO tree, please see Figs S2 and S3.

et al., 2013). Hence, TRPC1 and other ion channels such as TRPM7, are involved in very specific aspects of EMT remodelling and may therefore function as fine-tuners of EMT induction. They therefore represent opportunities to therapeutically target specific aspects of the mesenchymal phenotype in breast cancer.

TRPC1 silencing inhibited hypoxia- but not EGF-mediated stimulation of EGFR(Y1172) and STAT3(Y705) phosphorylation. Specific regulation by TRPC1 of hypoxia but not EGF responses, indicated that this channel is not just a simple regulator of Ca^{2+}-dependent housekeeping functions required for activation of the EGFR and STAT3 signalling pathways. Instead, TRPC1 is a specific regulator of processes associated with the transactivation of EGFR during hypoxia, which occurs through a HIF1α-independent mechanism. We also demonstrated that TRPC1-mediated regulation of EGFR activity during hypoxia is manifest as effects on the autophagy marker LC3B (Fig. 6). In A549 lung carcinoma cells, *TRPC1* silencing inhibits EGF-induced phosphoryation of EGFR at a different phosphorylation site (Y1068) (Tajeddine and Gailly, 2012), suggesting that TRPC1 selectively regulates signalling cascades through differential control of autophosphorylation sites (Nyati et al., 2006) and/or cell-type-specific roles for TRPC1 in EGFR signalling. Cell-type-specific roles for TRPC1 are also reflected in the regulation of store-operated Ca^{2+} entry (Cheng et al., 2013; Davis et al., 2012). Indeed, in A549 but not MDA-MB-468 cells, TRPC1 is a regulator of store-operated Ca^{2+} entry (Davis et al., 2012; Tajeddine and Gailly, 2012). This highly context-dependent role for TRPC1 in store-operated Ca^{2+} entry may explain the major differences in phenotypes between *Trpc1*- and *Orai1* (the classical store-operated Ca^{2+} entry component)-knockout mice: *Orai1*-null mice are associated with much more severe effects than *Trpc1*-knockout mice (Liu et al., 2007), including compromised immunity (Kim et al., 2011) and defects in osteoblast function (Robinson et al., 2012). TRPC1 is not the only Ca^{2+}-influx pathway where its contribution is dependent upon the cell identity because silencing of *ORAI3* inhibits store-operated Ca^{2+} entry in oestrogen-receptor-positive but not oestrogen-negative breast cancer cell lines (Motiani et al., 2010).

TRPC1 is not responsible for store-operated Ca^{2+} entry in either normoxia (Davis et al., 2012) or after hypoxia in MDA-MB-468 breast cancer cells; indeed, *TRPC1* silencing produces a modest increase in store-operated Ca^{2+} entry. However, our studies do show that TRPC1 is a major regulator of non-stimulated Ca^{2+} influx after hypoxia. The contribution of TRPC1 on basal $[Ca^{2+}]_{CYT}$ is associated with the pathogenesis of chronic hypoxia-induced pulmonary hypertension (Wang et al., 2015) and in cardiac myocytes, where the contribution of TRPC1 with TRPC4 to basal Ca^{2+} influx plays an important role in the development of cardiac hypertrophy (Camacho Londoño et al., 2015). TRPC1-mediated basal influx of Ca^{2+} in MDA-MB-468 breast cancer cells appears to be a trigger for the normoxic expression of HIF1α expression via a PTEN–Akt-dependent pathway.

Mutations in the PTEN tumour supressor gene are a characteristic of a variety of tumour types (Li et al., 1997), and in breast cancer they are associated with metastasis and poor prognosis (Saal et al., 2005, 2007). Loss of PTEN is a well characterised inducer of HIF1α expression in the absence of hypoxia, via enhancement of Akt activity (deGraffenried et al., 2004; Pore et al., 2006); however, the potential role of Ca^{2+} signalling in this process has not been fully explored. Our studies in PTEN-deficient MDA-MB-468 breast cancer cells showed that *TRPC1* silencing almost completely abolished the expression of HIF1α under normoxic conditions, as well as basal Akt but not basal EGFR or STAT3 phosphorylation. The association between TRPC1 and the Akt–HIF1α axis (Pore et al., 2006) was further supported by the inhibition of basal HIF1α expression in MDA-MB-468 breast cancer cells with pharmacological inhibition of Akt, the reduction in Akt phosphorylation and HIF1α levels in HCC1569 cells with *TRPC1* silencing, and the role of TRPC1 downregulation and Akt inhibition in neurotoxin-induced ER stress in dopaminergic neurons reported by Selvaraj et al. (2012). Given that *Trpc1*-null mouse phenotypes have been described as not dramatic (Nilius and Szallasi, 2014) and include modest body weight increases, defective saliva secretion (Liu et al., 2007; Nilius and Szallasi, 2014) and altered recovery from anaphylaxis (Medic et al., 2013), targeting TRPC1

Journal of Cell Science (2017) 130, 2292-2305 doi:10.1242/jcs.196659

may offer a unique mechanism to regulate some of the cellular events associated with PTEN loss in some cancers without global systemic toxicity.

In conclusion, this study provides new insights into changes in TRPC ion channels that are associated with hypoxia in breast cancer cells and the role of TRPC1 in these processes. The contribution of TRPC1 is dependent on specific oncogenic mutations such as the tumour suppressor PTEN and the recruitment of HIF1α-dependent and -independent pathways. This new understanding of the role of TRPC1 in the response of breast cancer cells to hypoxia may enable more effective targeting of cancer metastasis and/or survival mechanisms.

MATERIALS AND METHODS

Cell culture and induction of hypoxia

MDA-MB-468 and MDA-MB-231 human breast cancer cell lines were obtained from The Brisbane Breast Bank, UQCCR, Australia and American Type Culture Collection (ATCC) respectively, and cultured and maintained as previously described (Azimi et al., 2015, 2017). HCC1569 cells were obtained from the ATCC and maintained in RPMI 1640 medium (Sigma-Aldrich) supplemented with 10% FBS at 37°C and 5% CO_2. For hypoxia studies, 24 h post plating MDA-MB-468 breast cancer cells were serum reduced (0.5% FBS, 24 h) and then maintained in 1% O_2, 5% CO_2 and 94% N_2 for periods stated in results. For studies of EGF-induced EMT, cells were serum reduced (0.5% FBS, 24 h) 24 h post plating and then treated with 50 ng ml^{-1} EGF (E9644; Sigma-Aldrich) for stated periods. Cell lines were routinely tested to confirm the absence of mycoplasma (MycoAlert). STR profiling was performed using the StemElite ID Profiling Kit (Promega).

Quantitative real-time PCR

Total RNA was isolated and purified from cultured cells using an RNeasy Plus Mini Kit (74134; Qiagen). cDNA was synthesised using an Omniscript RT Kit (205111, Qiagen) and was amplified using TaqMan Fast Universal PCR Master Mix (4352042; Applied Biosystems) and TaqMan gene expression assays in a StepOnePlus instrument (Applied Biosystems) under universal cycling conditions. The relative target quantity was determined using the comparative CT (ΔΔCT) method by normalising to 18S rRNA as previously described (Aung et al., 2009). The TaqMan gene expression assays used in this study included: vimentin (Hs00185584_m1), Twist (Hs00361186_m1), Snail (Hs00195591_m1), N-cadherin (Hs00983062_m1), claudin-4 (Hs00976831_s1), HIF-1α (Hs00153153_m1), TRPC1 (Hs00608195_m1), TRPC3 (Hs00162985_m1), TRPC4 (Hs01077392_m1), TRPC5 (Hs00202960_m1), TRPC6 (Hs00989190_m1), TRPC7 (Hs00220638_m1), STAT3 (Hs00374280_m1) and EGFR (Hs01076092_m1).

Immunoblotting

Cells were lysed in protein lysis buffer supplemented with protease and phosphatase inhibitors (Roche Applied Science). Samples were resolved on NuPAGE Novex 4-12% BisTris gels (Invitrogen) or Mini-Protean TGX Stain-Free Precast Gels (Bio-Rad) and transferred to a PVDF membrane. The following primary antibodies were purchased from Cell Signaling and were diluted 1:1000: phospho-Akt (Ser473) (4051), Akt (9272), EGFR (2232), phospho-EGFR (Tyr1173) (4407), STAT3 (9139) and phospho-STAT3 (Tyr705). Anti-HIF-1α antibody was purchased from BD Bioscience (610959, 1:500 dilution) and β-actin antibody was purchased from Sigma-Aldrich (A5441, 1:10,000 dilution). HRP-conjugated secondary antibodies goat anti-mouse (170-6516) and goat anti-rabbit (170-6516) were purchased from Bio-Rad and used at a 1:10,000 dilution. Primary antibodies were incubated with membrane overnight at 4°C and secondary antibodies for 1 h at room temperature. Chemiluminescence blots were imaged using a Bio-Rad VersaDoc Imaging System or a Bio-Rad ChemiDoc Imaging System. Bands were quantified by Quantity One (v.4.6.7, Bio-Rad) and normalised to β-actin. Phosphorylated proteins were then quantified relative to their total protein. Results are expressed as fraction of total protein band intensity.

siRNA transfection

Dharmacon ON-TARGETplus SMARTpool siRNA (100 nmol per well) and DharmaFECT4 Transfection Reagent (0.1 µl per well) were used for siRNA silencing (GE Dharmacon). The following ON-TARGETplus SMARTpool siRNAs were used in this study: *TRPC1* (L-004191-00), *HIF1A* (L-004018-00), *EGFR* (L-003114-00) and *STAT3* (L-003544-00). MDA-MB-468 cells were seeded at 6×10^4 (48 h hypoxia) or 1×10^5 (6 h and 24 h hypoxia) cells per well in a 96-well plate. Post plating (24 h), cells were transfected with siRNA for 48 h. Cells were then serum starved (0.5% FBS) for 24 h and exposed to hypoxic conditions (1% O_2) for the indicated time periods. For experiments involving *TRPC1* silencing in HCC1569 cells, 5000 cells per well were seeded in a 96-well plate and left to adhere for 24 h. Cells were then treated with *TRPC1* siRNA for 48 h and were subsequently serum deprived (0.5% FBS). After 24 h cells in serum-deprived medium, cells were treated with 0.1% DMSO in serum-deprived medium for 24 h, 0.5 µM acetic acid was added for 20 min, before addition of cell lysis buffer for protein isolation

Additional experiments with different siRNAs (Dharmacon siGENOME) are presented in Fig. S6A,B. The following Dharmacon siGENOME siRNAs were used in this study: non-targeting (D-001206-14-05) and *TRPC1* (M-004191-02). Effectiveness of each siRNA was confirmed through greater than 80% silencing of the relevant target gene as quantified using real-time RT-PCR.

Akt pharmacological inhibition

For pharmacological inhibition studies, cells were seeded at 2×10^5 cells per well (96-well plate) and left to adhere for 24 h before serum deprivation (0.5% FBS) for a further 24 h. Cells were then incubated with Akt inhibitor MK-2206 2HCl or vehicle control (0.05% DMSO) for 24 h.

Measurement of intracellular free Ca^{2+}

Cytosolic free Ca^{2+} ($[Ca^{2+}]_{CYT}$) was assessed using a Fluorometric Imaging Plate Reader ($FLIPR^{TETRA}$, Molecular Devices) and the BD PBX no-wash Ca^{2+} Assay Kit (BD Biosciences) as described previously (Grice et al., 2010). Cells were seeded at 1×10^4 cells per well in 96-well black plates (Corning Costar). *TRPC1* and *HIF1A* were silenced using siRNA as described above. Post hypoxia (24 h), cells were loaded for 60 min at 37°C with 2 µM PBX Ca^{2+} indicator dye in a solution comprising 5% (v/v) PBX Signal Enhancer and 500 µM probenecid in physiological salt solution (PSS; 5.9 mM KCl, 1.4 mM MgCl2, 10 mM HEPES, 1.2 mM NaH_2PO_4, 5 mM $NaHCO_3$, 140 mM NaCl, 11.5 mM glucose, 1.8 mM $CaCl_2$). For assessment of store-operated Ca^{2+} entry, BAPTA (500 µM, Invitrogen) was added (for chelation of extracellular Ca^{2+}) followed by the addition of cyclopiazonic acid (10 µM, Sigma) [for inhibition of sarco/endoplasmic reticulum Ca^{2+}-ATPases (SERCA) pump and subsequent depletion of ER Ca^{2+}]. Store-operated Ca^{2+} influx was assessed by the addition of $CaCl_2$ (0.6 mM) 700 s after the addition of cyclopiazonic acid. For the assessment of non-stimulated Ca^{2+} influx, following addition of BAPTA, 0.6 mM $CaCl_2$ was added in the absence of cyclopiazonic acid. Fluorescence was assessed at 470-495 nm excitation and 515-575 nm emission wavelengths. Data analyses were performed using ScreenWorks Software (v.2.0.0.27, Molecular Devices). Fluorescence response over baseline was assessed as a relative measure of $[Ca^{2+}]_{CYT}$.

TRPC1 plasmid DNA transfection

TRPC1 plasmid was distributed by Addgene and was originally donated by Craig Montell (Addgene plasmid # 24408) (Xu et al., 1997). The pcDNA3.1 vector was used for a control. MDA-MB-468 cells (4×10^5 cells) were transfected with 1.2 µg plasmids in a 20 µl solution of SE Cell Line Kit (Lonza) using DS-120 programme of a 4D-Nucleofector unit (Lonza) and subsequently plated in 96-well plates.

Analysis of *TRPC1* expression in breast cancer cell lines

For analyses of the *TRPC1* gene expression profile across a panel of breast cancer cell lines, we used a publically available microarray dataset from Array Express (accession no. E-MTAB-181) (Heiser et al., 2012) representing three subgroups of Luminal (predominantly luminal;

Journal of Cell Science

corresponding to luminal and HER2 breast cancer subtypes), basal A (mixed basal/luminal; corresponding to basal breast cancer subtype) and basal B (corresponding to mesenchymal subgroup with increased invasive properties; corresponding to claudin-low breast cancer subtype) (Neve et al., 2006; Prat et al., 2010).

Analysis of *TRPC1* expression in breast tumours

Breast tumour gene expression data were sourced from the University of North Carolina (UNC) cohort (Harrell et al., 2012). The UNC dataset classified its 855 tumours into the five intrinsic PAM50 molecular subtypes and further sub-divided the basal-like and normal-like subtypes into claudin-low tumours, basal-like (basal, 140), claudin-low (C-Low, 90), HER2-enriched (HER2, 144), luminal A (LumA, 243), luminal B (LumB, 162) and normal-like (N-Like, 76). Triple-negative breast cancers (TNBCs) from the UNC cohort [based on immunohistochemistry (IHC) of the oestrogen (ER) and progesterone receptors (PR) and HER2] were assigned a TNBC subtype based on the expression of subtype-specific gene signatures (Burstein et al., 2015). This analysis classified the 200 TNBCs into 83 basal-like immune-activated (BLIA), 95 basal-like immune-suppressed (BLIS), 6 luminal androgen receptor (LAR) and 16 mesenchymal (MES).

Survival analysis of basal tumours and association with *TRPC1* levels

The online tool, Kaplan–Meier plotter (Győrffy et al., 2010) was utilised to produce survival curves for breast cancer patients. Two cohorts were used in this study, all patients with basal tumours and patients with basal tumours and classified as lymph-node positive (N+). Patient relapse-free survival (RFS) was stratified based on *TRPC1* (Affymetrix probe ID: 205802_at) expression using the 'Auto select best cutoff,' feature. Patient numbers in the low and high expression groups are displayed on the graphs, as are their hazard ratios (HRs) and *P*-values.

Identification of genes most correlated to *TRPC1* expression in breast cancers

The top 100 genes positively and negatively correlated to *TRPC1* expression were sourced from TCGA microarray data (available at www.cbioportal.org) (Cerami et al., 2012; Gao et al., 2013; Koboldt et al., 2012). This dataset contains 463 tumours with microarray expression data. Correlations to *TRPC1* expression were calculated through both Pearson and Spearman methodologies, Pearson was used as a cut-off for the top 100. For the complete list of positive and negative correlated genes, please see Tables S1 and S2, respectively.

Gene ontology analysis

The top 100 genes positively and negatively correlated to *TRPC1* expression were input into the online tool WEB-based GEne SeT AnaLysis Toolkit (WebGestalt, http://bioinfo.vanderbilt.edu/webgestalt/) (Wang et al., 2013). Gene ontology (GO) results from this analysis were determined as significant based on an adjusted *P*-value for multiple testing (Benhamini and Hochberg method) of a hypergeometric test (raw *P*-value) with a significance cut-off level of 0.05 and a minimum of 2 genes allocated to the GO term. GO hierarchical trees produced from this analysis are available in Figs S7 and S8, and summarised in Table 1.

TRPC1 promoter analysis

Genomic data for human mammary epithelial cell (HMEC) histone methylation was sourced from ENCODE through the IGV browser (Dunham et al., 2012; Robinson et al., 2011). Both Phastcons and CpG islands were sourced from the Broad Institute data registry (http://data.broadinstitute.org/igvdata/$$_dataServerRegistry.txt, accessed through IGV http://software.broadinstitute.org/software/igv Version 2.3.81). Mapped HIF1 ChIP-Seq data was sourced from GSE59937 (Zhang et al., 2015). The HIF1 motif (RCGTGM) was sourced from Schödel et al. (2011). Relevant data was then loaded into the Integrative genomics viewer (IGV, Mac desktop application v.2.3.81; Robinson et al., 2011) and a snapshot taken of human chromosome 3:142,442,229-142,445,500, build hg19.

Statistical analysis

Statistical analysis was performed using GraphPad Prism v.6.05 for Windows (GraphPad software). Details of each test employed are described in each figure legend. Data are presented as mean±s.d.

Competing interests

G.R.M. and S.J.R.-T. are associated with QUE Oncology Inc.

Author contributions

Conceptualization: I.A., M.A.B., E.T., S.J.R.-T., G.R.M.; Methodology: I.A., M.J.G.M., E.K., D.T., K.I.D.S.Y.; Software: I.A., M.J.G.M.; Validation: I.A.; Formal analysis: I.A., M.J.G.M., E.K., D.T., K.I.D.S.Y.; Investigation: I.A., M.J.G.M., E.K., D.T., K.I.D.S.Y.; Data curation: I.A.; Writing – original draft: I.A., M.J.G.M., E.K., S.J.R.-T., G.R.M.; Writing – review and editing: I.A., M.J.G.M., E.K., D.T., K.I.D.S.Y., M.A.B., E.T., S.J.R.-T., G.R.M.; Visualization: I.A.; Supervision: M.A.B., S.J.R.-T., G.R.M.; Project administration: S.J.R.-T., G.R.M.; Funding acquisition: S.J.R.-T., G.R.M.

Funding

The research was supported by the National Health and Medical Research Council (NHMRC; project grants 569645 and 1022263) and the Cancer Council Queensland (1042819). G.R.M. is supported by the Mater Foundation. E.W.T. was funded in part by the EM*Pathy* Breast Cancer Network of the National Breast Cancer Foundation (NCBF) (CG-10-04), Australia. The Translational Research Institute is supported by a grant from the Australian Government. The NBCF also supported the research conducted by M.J.G.M. and M.A.B. (CG-12-07).

Supplementary information

Supplementary information available online at
http://jcs.biologists.org/lookup/doi/10.1242/jcs.196659.supplemental

References

Aung, C. S., Ye, W., Plowman, G., Peters, A. A., Monteith, G. R. and Roberts-Thomson, S. J. (2009). Plasma membrane calcium ATPase 4 and the remodeling of calcium homeostasis in human colon cancer cells. *Carcinogenesis* **30**, 1962-1969.

Azimi, I. and Monteith, G. R. (2016). Plasma membrane ion channels and epithelial to mesenchymal transition in cancer cells. *Endocr. Relat. Cancer* **23**, R517-R525.

Azimi, I., Beilby, H., Davis, F. M., Marcial, D. L., Kenny, P. A., Thompson, E. W., Roberts-Thomson, S. J. and Monteith, G. R. (2015). Altered purinergic receptor-Ca^{2+} signaling associated with hypoxia-induced epithelial-mesenchymal transition in breast cancer cells. *Mol. Oncol.* **10**, 166-178.

Azimi, I., Flanagan, J. U., Stevenson, R. J., Inserra, M., Vetter, I., Monteith, G. R. and Denny, W. A. (2017). Evaluation of known and novel inhibitors of Orai1-mediated store operated Ca^{2+} entry in MDA-MB-231 breast cancer cells using a Fluorescence Imaging Plate Reader assay. *Bioorg. Med. Chem.* **25**, 440-449.

Bissell, M. J. and Hines, W. C. (2011). Why don't we get more cancer? A proposed role of the microenvironment in restraining cancer progression. *Nat. Med.* **17**, 320-329.

Blick, T., Hugo, H., Widodo, E., Waltham, M., Pinto, C., Mani, S. A., Weinberg, R. A., Neve, R. M., Lenburg, M. E. and Thompson, E. W. (2010). Epithelial mesenchymal transition traits in human breast cancer cell lines parallel the CD44hi/CD24lo/- stem cell phenotype in human breast cancer. *J. Mammary Gland Biol. Neoplasia* **15**, 235-252.

Burstein, M. D., Tsimelzon, A., Poage, G. M., Coyington, K. R., Contreras, A., Fuqua, S. A. W., Sayage, M. I., Osborne, C. K., Hilsenbeck, S. G., Chang, J. C. et al. (2015). Comprehensive genomic analysis identifies novel subtypes and targets of triple-negative breast cancer. *Clin. Cancer Res.* **21**, 1688-1698.

Camacho Londoño, J. E., Tian, Q. H., Hammer, K., Schröder, L., Camacho Londoño, J., Reil, J. C., He, T., Oberhofer, M., Mannebach, S., Mathar, I. et al. (2015). A background Ca^{2+} entry pathway mediated by TRPC1/TRPC4 is critical for development of pathological cardiac remodelling. *Eur. Heart J.* **36**, 2257-2266.

Cantley, L. C. and Neel, B. G. (1999). New insights into tumor suppression: PTEN suppresses tumor formation by restraining the phosphoinositide 3-kinase AKT pathway. *Proc. Natl. Acad. Sci. USA* **96**, 4240-4245.

Cárdenas, C., Miller, R. A., Smith, I., Bui, T., Molgó, J., Müller, M., Vais, H., Cheung, K.-H., Yang, J., Parker, I. et al. (2010). Essential regulation of cell bioenergetics by constitutive InsP3 receptor Ca^{2+} transfer to mitochondria. *Cell* **142**, 270-283.

Cerami, E., Gao, J., Dogrusoz, U., Gross, B. E., Sumer, S. O., Aksoy, B. A., Jacobsen, A., Byrne, C. J., Heuer, M. L., Larsson, E. et al. (2012). The cBio cancer genomics portal: an open platform for exploring multidimensional cancer genomics data. *Cancer Discov.* **2**, 401-404.

Cheng, K. T., Ong, H. L., Liu, X. and Ambudkar, I. S. (2013). Contribution and regulation of TRPC channels in store-operated Ca^{2+} entry. *Curr. Top. Membr.* **71**, 149-179.

Chou, C.-C., Chou, M.-J. and Tzen, C.-Y. (2009). PIK3CA mutation occurs in nasopharyngeal carcinoma but does not significantly influence the disease-specific survival. *Med. Oncol.* **26**, 322-326.
Cooke, V. G., LeBleu, V. S., Keskin, D., Khan, Z., O'Connell, J. T., Teng, Y., Duncan, M. B., Xie, L., Maeda, G., Vong, S. et al. (2012). Pericyte depletion results in hypoxia-associated epithelial-to-mesenchymal transition and metastasis mediated by met signaling pathway. *Cancer Cell* **21**, 66-81.
Cui, Y., Li, Y. Y., Li, J., Zhang, H. Y., Wang, F., Bai, X. and Li, S. S. (2016). STAT3 regulates hypoxia-induced epithelial mesenchymal transition in oesophageal squamous cell cancer. *Oncol. Rep.* **36**, 108-116.
Davis, F. M., Peters, A. A., Grice, D. M., Cabot, P. J., Parat, M.-O., Roberts-Thomson, S. J. and Monteith, G. R. (2012). Non-stimulated, agonist-stimulated and store-operated Ca^{2+} influx in MDA-MB-468 breast cancer cells and the effect of EGF-induced EMT on calcium entry. *PLoS ONE* **7**, e36923.
Davis, F. M., Azimi, I., Faville, R. A., Peters, A. A., Jalink, K., Putney, J. W., Jr, Goodhill, G. J., Thompson, E. W., Roberts-Thomson, S. J. and Monteith, G. R. (2013). Induction of epithelial-mesenchymal transition (EMT) in breast cancer cells is calcium signal dependent. *Oncogene* **33**, 2307-2316.
Decuypere, J. P., Kindt, D., Luyten, T., Welkenhuyzen, K., Missiaen, L., De Smedt, H., Bultynck, G. and Parys, J. B. (2013). mTOR-controlled autophagy requires intracellular Ca^{2+} signaling. *PLoS ONE* **8**, e61020.
deGraffenried, L. A., Fulcher, L., Friedrichs, W. E., Grunwald, V., Ray, R. B. and Hidalgo, M. (2004). Reduced PTEN expression in breast cancer cells confers susceptibility to inhibitors of the PI3 kinase/Akt pathway. *Ann. Oncol.* **15**, 1510-1516.
Dunham, I. Kundaje, A. Aldred, S. F. Collins, P. J. Davis, C. A., Doyle, F. Epstein, C. B. Frietze, S. Harrow, J. Kaul, R. et al. (2012). An integrated encyclopedia of DNA elements in the human genome. *Nature* **489**, 57-74.
Fischer, K. R., Durrans, A., Lee, S., Sheng, J. T., Li, F. H., Wong, S. T. C., Choi, H. J., El Rayes, T., Ryu, S. H., Troeger, J. et al. (2015). Epithelial-to-mesenchymal transition is not required for lung metastasis but contributes to chemoresistance. *Nature* **527**, 472-476.
Gao, J. J., Aksoy, B. A., Dogrusoz, U., Dresdner, G., Gross, B., Sumer, S. O., Sun, Y. C., Jacobsen, A., Sinha, R., Larsson, E. et al. (2013). Integrative analysis of complex cancer genomics and clinical profiles using the cBioPortal. *Sci. Signal.* **6**, pl1.
Grice, D. M., Vetter, I., Faddy, H. M., Kenny, P. A., Roberts-Thomson, S. J. and Monteith, G. R. (2010). Golgi calcium pump secretory pathway calcium ATPase 1 (SPCA1) is a key regulator of insulin-like growth factor receptor (IGF1R) processing in the basal-like breast cancer cell line MDA-MB-231. *J. Biol. Chem.* **285**, 37458-37466.
Győrffy, B., Lanczky, A., Eklund, A. C., Denkert, C., Budczies, J., Li, Q. and Szallasi, Z. (2010). An online survival analysis tool to rapidly assess the effect of 22,277 genes on breast cancer prognosis using microarray data of 1,809 patients. *Breast Cancer Res. Treat.* **123**, 725-731.
Harrell, J. C., Prat, A., Parker, J. S., Fan, C., He, X., Carey, L., Anders, C., Ewend, M. and Perou, C. M. (2012). Genomic analysis identifies unique signatures predictive of brain, lung, and liver relapse. *Breast Cancer Res. Treat.* **132**, 523-535.
Heiser, L. M., Sadanandam, A., Kuo, W.-L., Benz, S. C., Goldstein, T. C., Ng, S., Gibb, W. J., Wang, N. J., Ziyad, S., Tong, F. et al. (2012). Subtype and pathway specific responses to anticancer compounds in breast cancer. *Proc. Natl. Acad. Sci. USA* **109**, 2724-2729.
Hennessy, B. T., Gonzalez-Angulo, A.-M., Stemke-Hale, K., Gilcrease, M. Z., Krishnamurthy, S., Lee, J.-S., Fridlyand, J., Sahin, A., Agarwal, R., Joy, C. et al. (2009). Characterization of a naturally occurring breast cancer subset enriched in epithelial-to-mesenchymal transition and stem cell characteristics. *Cancer Res.* **69**, 4116-4124.
Hu, Y.-L., DeLay, M., Jahangiri, A., Molinaro, A. M., Rose, S. D., Carbonell, W. S. and Aghi, M. K. (2012). Hypoxia-induced autophagy promotes tumor cell survival and adaptation to antiangiogenic treatment in glioblastoma. *Cancer Res.* **72**, 1773-1783.
Kaczmarek, J. S., Riccio, A. and Clapham, D. E. (2012). Calpain cleaves and activates the TRPC5 channel to participate in semaphorin 3A-induced neuronal growth cone collapse. *Proc. Natl. Acad. Sci. USA* **109**, 7888-7892.
Kheradpezhouh, E., Ma, L. L., Morphett, A., Barritt, G. J. and Rychkov, G. Y. (2014). TRPM2 channels mediate acetaminophen-induced liver damage. *Proc. Natl. Acad. Sci. USA* **111**, 3176-3181.
Kim, K.-D., Srikanth, S., Yee, M.-K. W., Mock, D. C., Lawson, G. W. and Gwack, Y. (2011). ORAI1 deficiency impairs activated T cell death and enhances T cell survival. *J. Immunol.* **187**, 3620-3630.
Koboldt, D. C. Fulton, R. S. McLellan, M. D. Schmidt, H. Kalicki-Veizer, J. McMichael, J. F. Fulton, L. L. Dooling, D. J. Ding, L. Mardis, E. R. et al. (2012). Comprehensive molecular portraits of human breast tumours. *Nature* **490**, 61-70.
Kondratov, K. A., Chernorudskiy, A. L., Amosova, A. P. and Kornilova, E. S. (2010). Termination of tyrphostin AG1478 application results in different recovery of EGF receptor tyrosine residues 1045 and 1173 phosphorylation in A431 cells. *Cell Biol. Int.* **34**, 81-87.
Kondratskyi, A., Yassine, M., Kondratska, K., Skryma, R., Slomianny, C. and Prevarskaya, N. (2013). Calcium-permeable ion channels in control of autophagy and cancer. *Front. Physiol.* **4**, 272.
Lester, R. D., Jo, M., Montel, V., Takimoto, S. and Gonias, S. L. (2007). uPAR induces epithelial-mesenchymal transition in hypoxic breast cancer cells. *J. Cell Biol.* **178**, 425-436.
Li, J., Yen, C., Liaw, D., Podsypanina, K., Bose, S., Wang, S. I., Puc, J., Miliaresis, C., Rodgers, L., McCombie, R. et al. (1997). PTEN, a putative protein tyrosine phosphatase gene mutated in human brain, breast, and prostate cancer. *Science* **275**, 1943-1947.
Liu, X. B., Cheng, K. T., Bandyopadhyay, B. C., Pani, B., Dietrich, A., Paria, B. C., Swaim, W. D., Beech, D., Yildrim, E., Singh, B. B. et al. (2007). Attenuation of store-operated Ca^{2+} current impairs salivary gland fluid secretion in TRPC1(-/-) mice. *Proc. Natl. Acad. Sci. USA* **104**, 17542-17547.
Lo, H.-W., Hsu, S.-C., Xia, W. Y., Cao, X. Y., Shih, J.-Y., Wei, Y. K., Abbruzzese, J. L., Hortobagyi, G. N. and Hung, M.-C. (2007). Epidermal growth factor receptor cooperates with signal transducer and activator of transcription 3 to induce epithelial-mesenchymal transition in cancer cells via up-regulation of TWIST gene expression. *Cancer Res.* **67**, 9066-9076.
Ma, X., Cai, Y., He, D., Zou, C., Zhang, P., Lo, C. Y., Xu, Z., Chan, F. L., Yu, S., Chen, Y. et al. (2012). Transient receptor potential channel TRPC5 is essential for P-glycoprotein induction in drug-resistant cancer cells. *Proc. Natl. Acad. Sci. USA* **109**, 16282-16287.
Ma, X., Chen, Z., Hua, D., He, D., Wang, L., Zhang, P., Wang, J., Cai, Y., Gao, C., Zhang, X. et al. (2014). Essential role for TrpC5-containing extracellular vesicles in breast cancer with chemotherapeutic resistance. *Proc. Natl. Acad. Sci. USA* **111**, 6389-6394.
Malczyk, M., Veith, C., Fuchs, B., Hofmann, K., Storch, U., Schermuly, R. T., Witzenrath, M., Ahlbrecht, K., Fecher-Trost, C., Flockerzi, V. et al. (2013). Classical transient receptor potential channel 1 in hypoxia-induced pulmonary hypertension. *Am. J. Respir. Crit. Care Med.* **188**, 1451-1459.
Medic, N., Desai, A., Olivera, A., Abramowitz, J., Birnbaumer, L., Beaven, M. A., Gilfillan, A. M. and Metcalfe, D. D. (2013). Knockout of the Trpc1 gene reveals that TRPC1 can promote recovery from anaphylaxis by negatively regulating mast cell TNF-alpha production. *Cell Calcium* **53**, 315-326.
Misra, A., Pandey, C., Sze, S. K. and Thanabalu, T. (2012). Hypoxia activated EGFR signaling induces epithelial to mesenchymal transition (EMT). *PLoS ONE* **7**, e49766.
Motiani, R. K., Abdullaev, I. F. and Trebak, M. (2010). A novel native store-operated calcium channel encoded by Orai3 selective requirement of Orai3 versus Orai1 in estrogen receptor-positive versus estrogen receptor-negative breast cancer cells. *J. Biol. Chem.* **285**, 19173-19183.
Neve, R. M., Chin, K., Fridlyand, J., Yeh, J., Baehner, F. L., Fevr, T., Clark, L., Bayani, N., Coppe, J.-P., Tong, F. et al. (2006). A collection of breast cancer cell lines for the study of functionally distinct cancer subtypes. *Cancer Cell* **10**, 515-527.
Nilius, B. and Szallasi, A. (2014). Transient receptor potential channels as drug targets: from the science of basic research to the art of medicine. *Pharmacol. Rev.* **66**, 676-814.
Nyati, M. K., Morgan, M. A., Feng, F. Y. and Lawrence, T. S. (2006). Integration of EGFR inhibitors with radiochemotherapy. *Nat. Rev. Cancer* **6**, 876-885.
Ortiz-Barahona, A., Villar, D., Pescador, N., Amigo, J. and del Peso, L. (2010). Genome-wide identification of hypoxia-inducible factor binding sites and target genes by a probabilistic model integrating transcription-profiling data and in silico binding site prediction. *Nucleic Acids Res.* **38**, 2332-2345.
Parys, J. B., Decuypere, J.-P. and Bultynck, G. (2012). Role of the inositol 1,4,5-trisphosphate receptor/Ca^{2+}-release channel in autophagy. *Cell Commun. Signal.* **10**, 17.
Pawlus, M. R., Wang, L. and Hu, C.-J. (2014). STAT3 and HIF1alpha cooperatively activate HIF1 target genes in MDA-MB-231 and RCC4 cells. *Oncogene* **33**, 1670-1679.
Peng, X.-H., Karna, P., Cao, Z. H., Jiang, B. H., Zhou, M. X. and Yang, L. (2006). Cross-talk between epidermal growth factor receptor and hypoxia-inducible factor-1 alpha signal pathways increases resistance to apoptosis by up-regulating survivin gene expression. *J. Biol. Chem.* **281**, 25903-25914.
Pore, N., Jiang, Z. B., Shu, H. K., Bernhard, E., Kao, G. D. and Maity, A. (2006). Akt1 activation can augment hypoxia-inducible factor-1 alpha expression by increasing protein translation through a mammalian target of rapamycin-independent pathway. *Mol. Cancer Res.* **4**, 471-479.
Prat, A., Parker, J. S., Karginova, O., Fan, C., Livasy, C., Herschkowitz, J. I., He, X. and Perou, C. M. (2010). Phenotypic and molecular characterization of the claudin-low intrinsic subtype of breast cancer. *Breast Cancer Res.* **12**, R68.
Riccio, A., Li, Y., Moon, J., Kim, K.-S., Smith, K. S., Rudolph, U., Gapon, S., Yao, G. L., Tsvetkov, E., Rodig, S. J. et al. (2009). Essential role for TRPC5 in amygdala function and fear-related behavior. *Cell* **137**, 761-772.
Robinson, J. T., Thorvaldsdottir, H., Winckler, W., Guttman, M., Lander, E. S., Getz, G. and Mesirov, J. P. (2011). Integrative genomics viewer. *Nat. Biotechnol.* **29**, 24-26.
Robinson, L. J., Mancarella, S., Songsawad, D., Tourkova, I. L., Barnett, J. B., Gill, D. L., Soboloff, J. and Blair, H. C. (2012). Gene disruption of the calcium

channel Orai1 results in inhibition of osteoclast and osteoblast differentiation and impairs skeletal development. *Lab. Investig.* **92**, 1071-1083.

Saal, L. H., Holm, K., Maurer, M., Memeo, L., Su, T., Wang, X. M., Yu, J. S., Malmstrom, P. O., Mansukhani, M., Enoksson, J. et al. (2005). PIK3CA mutations correlate with hormone receptors, node metastasis, and ERBB2, and are mutually exclusive with PTEN loss in human breast carcinoma. *Cancer Res.* **65**, 2554-2559.

Saal, L. H., Johansson, P., Holm, K., Gruvberger-Saal, S. K., She, Q.-B., Maurer, M., Koujak, S., Ferrando, A. A., Malmstrom, P., Memeo, L. et al. (2007). Poor prognosis in carcinoma is associated with a gene expression signature of aberrant PTEN tumor suppressor pathway activity. *Proc. Natl. Acad. Sci. USA* **104**, 7564-7569.

Salceda, S. and Caro, J. (1997). Hypoxia-inducible factor 1 alpha (HIF-1 alpha) protein is rapidly degraded by the ubiquitin-proteasome system under normoxic conditions: its stabilization by hypoxia depends on redox-induced changes. *J. Biol. Chem.* **272**, 22642-22647.

Schödel, J., Oikonomopoulos, S., Ragoussis, J., Pugh, C. W., Ratcliffe, P. J. and Mole, D. R. (2011). High-resolution genome-wide mapping of HIF-binding sites by ChIP-seq. *Blood* **117**, e207-e217.

Selvaraj, S., Sun, Y., Watt, J. A., Wang, S., Lei, S., Birnbaumer, L. and Singh, B. B. (2012). Neurotoxin-Induced ER stress in mouse dopaminergic neurons involves downregulation of TRPC1 and inhibition of AKT/mTOR signaling. *J. Clin. Investig.* **122**, 1354-1367.

Selvendiran, K., Bratasz, A., Kuppusamy, M. L., Tazi, M. F., Rivera, B. K. and Kuppusamy, P. (2009). Hypoxia induces chemoresistance in ovarian cancer cells by activation of signal transducer and activator of transcription 3. *Int. J. Cancer* **125**, 2198-2204.

Semenza, G. L. (2013). Cancer-stromal cell interactions mediated by hypoxia-inducible factors promote angiogenesis, lymphangiogenesis, and metastasis. *Oncogene* **32**, 4057-4063.

Semenza, G. L. (2016). The hypoxic tumor microenvironment: A driving force for breast cancer progression. *Biochim. Biophys. Acta.* **1863**, 382-391.

Soria, J. C., Lee, H. Y., Lee, J. I., Wang, L., Issa, J. P., Kemp, B. L., Liu, D. D., Kurie, J. M., Mao, L. and Khuri, F. R. (2002). Lack of PTEN expression in non-small cell lung cancer could be related to promoter methylation. *Clin. Cancer Res.* **8**, 1178-1184.

Tajeddine, N. and Gailly, P. (2012). TRPC1 protein channel is major regulator of epidermal growth factor receptor signaling. *J. Biol. Chem.* **287**, 16146-16157.

Tomaskovic-Crook, E., Thompson, E. W. and Thiery, J. P. (2009). Epithelial to mesenchymal transition and breast cancer. *Breast Cancer Res.* **11**, 213.

Wang, J., Weigand, L., Lu, W., Sylvester, J. T., Semenza, G. L. and Shimoda, L. A. (2006). Hypoxia inducible factor 1 mediates hypoxia-induced TRPC expression and elevated intracellular Ca^{2+} in pulmonary arterial smooth muscle cells. *Circ. Res.* **98**, 1528-1537.

Wang, J., Duncan, D., Shi, Z. and Zhang, B. (2013). WEB-based GEne SeT AnaLysis Toolkit (WebGestalt): update 2013. *Nucleic Acids Res.* **41**, W77-W83.

Wang, J., Fu, X., Yang, K., Jiang, Q., Chen, Y., Jia, J., Duan, X., Wang, E. W., He, J., Ran, P. et al. (2015). Hypoxia inducible factor-1-dependent up-regulation of BMP4 mediates hypoxia-induced increase of TRPC expression in PASMCs. *Cardiovasc. Res.* **107**, 108-118.

Weidemann, A. and Johnson, R. S. (2008). Biology of HIF-1alpha. *Cell Death Differ.* **15**, 621-627.

Wu, L. J., Sweet, T. B. and Clapham, D. E. (2010). International union of basic and clinical pharmacology. LXXVI. Current progress in the mammalian TRP ion channel family. *Pharmacol. Rev.* **62**, 381-404.

Xia, Y., Yang, X.-R., Fu, Z., Paudel, O., Abramowitz, J., Birnbaumer, L. and Sham, J. S. K. (2014). Classical transient receptor potential 1 and 6 contribute to hypoxic pulmonary hypertension through differential regulation of pulmonary vascular functions. *Hypertension* **63**, 173-180.

Xu, X.-Z. S., Li, H.-S., Guggino, W. B. and Montell, C. (1997). Coassembly of TRP and TRPL produces a distinct store-operated conductance. *Cell* **89**, 1155-1164.

Ye, X. and Weinberg, R. A. (2015). Epithelial-mesenchymal plasticity: a central regulator of cancer progression. *Trends Cell Biol.* **25**, 675-686.

Yildirim, E. and Birnbaumer, L. (2007). TRPC2: molecular biology and functional importance. *Handb. Exp. Pharmacol.* **179**, 53-75.

Zhang, J., Wang, C., Chen, X., Takada, M., Fan, C., Zheng, X., Wen, H., Liu, Y., Wang, C., Pestell, R. G. et al. (2015). EglN2 associates with the NRF1-PGC1 alpha complex and controls mitochondrial function in breast cancer. *EMBO J.* **34**, 2953-2970.

Zundel, W., Schindler, C., Haas-Kogan, D., Koong, A., Kaper, F., Chen, E., Gottschalk, A. R., Ryan, H. E., Johnson, R. S., Jefferson, A. B. et al. (2000). Loss of PTEN facilitates HIF-1-mediated gene expression. *Genes Dev.* **14**, 391-396.

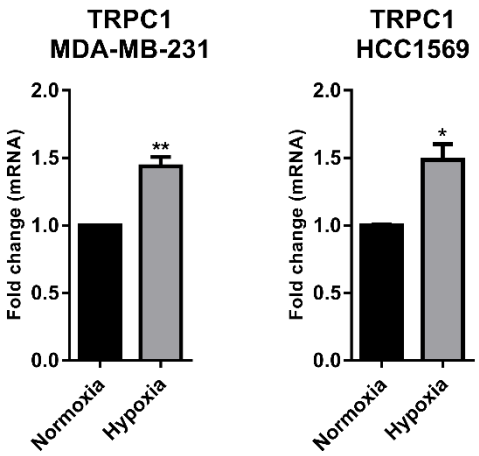

Fig. S1. TRPC1 mRNA expression is induced by hypoxia in MDA-MB-231 and HCC1569 breast cancer cells. *TRPC1* induction in MDA-MB-231 and HCC1569 cells 24 h after hypoxia. * $p < 0.01$, ** $p < 0.001$ compared with control (unpaired t-test), n = 3, mean ± SD

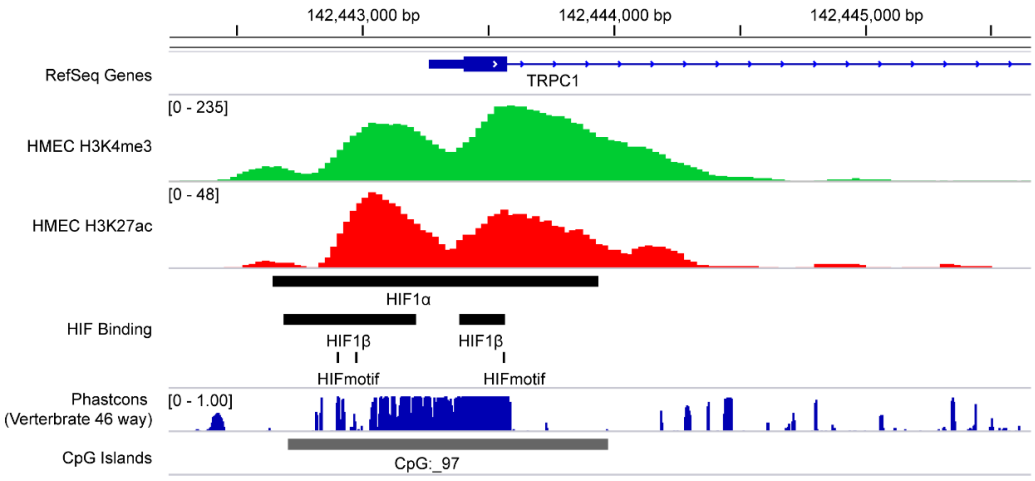

Fig. S2. HIF1 proteins bind the TRPC1 promoter in breast cancer cells. Snapshot from IGV of the genomic region of exon 1 for TRPC1, human chromosome 3. Displayed are the histone modifications associated with active promoters (HMEC), conservation (Phastcons), CpG islands, HIF ChIP-Seq peaks from MCF7 cells and instances of conserved HIF1 binding motifs.

Journal of Cell Science • Supplementary information

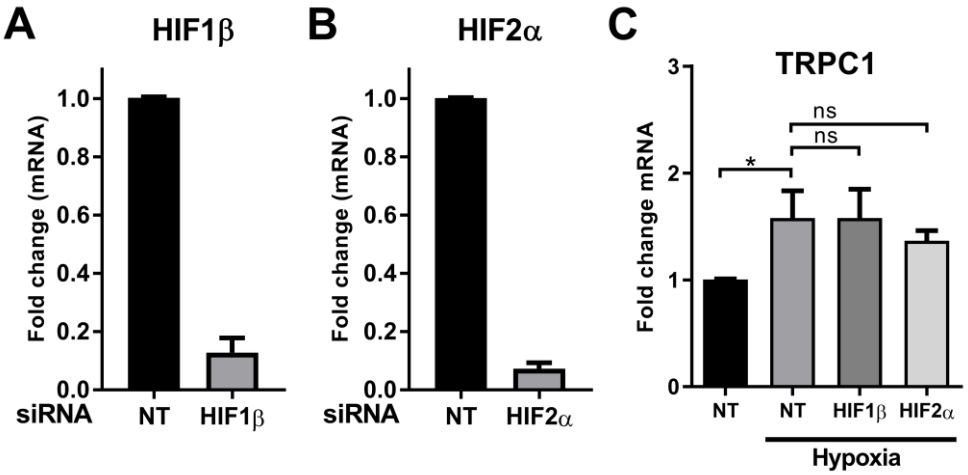

Fig. S3. Hypoxia-induced TRPC1 expression is not HIF1β- or HIF2α-sensitive. Confirmation of HIF1β (**A**) and HIF2α (**B**) siRNA-mediated silencing and (**C**) the effect of HIF1β and HIF2α silencing relative to non-targeting control (NT) on hypoxia-induced *TRPC1* mRNA up-regulation (24 h hypoxia). ns = not significant ($p > 0.05$) (one-way ANOVA, with Bonferroni's multiple comparisons), n = 3 ± SD.

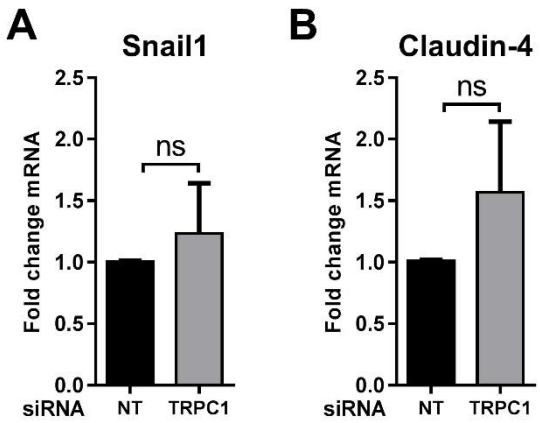

Figure S4. TRPC1 silencing has no significant effect on the basal levels of Snail1 and Claudin-4 in normoxia. The effect of TRPC1 silencing on basal levels of EMT markers Snail1 and Claudin-4 in MD-MB-468 cells. ns = not significant ($p > 0.05$) (unpaired t-test), n = 3, mean ± SD.

Journal of Cell Science • Supplementary information

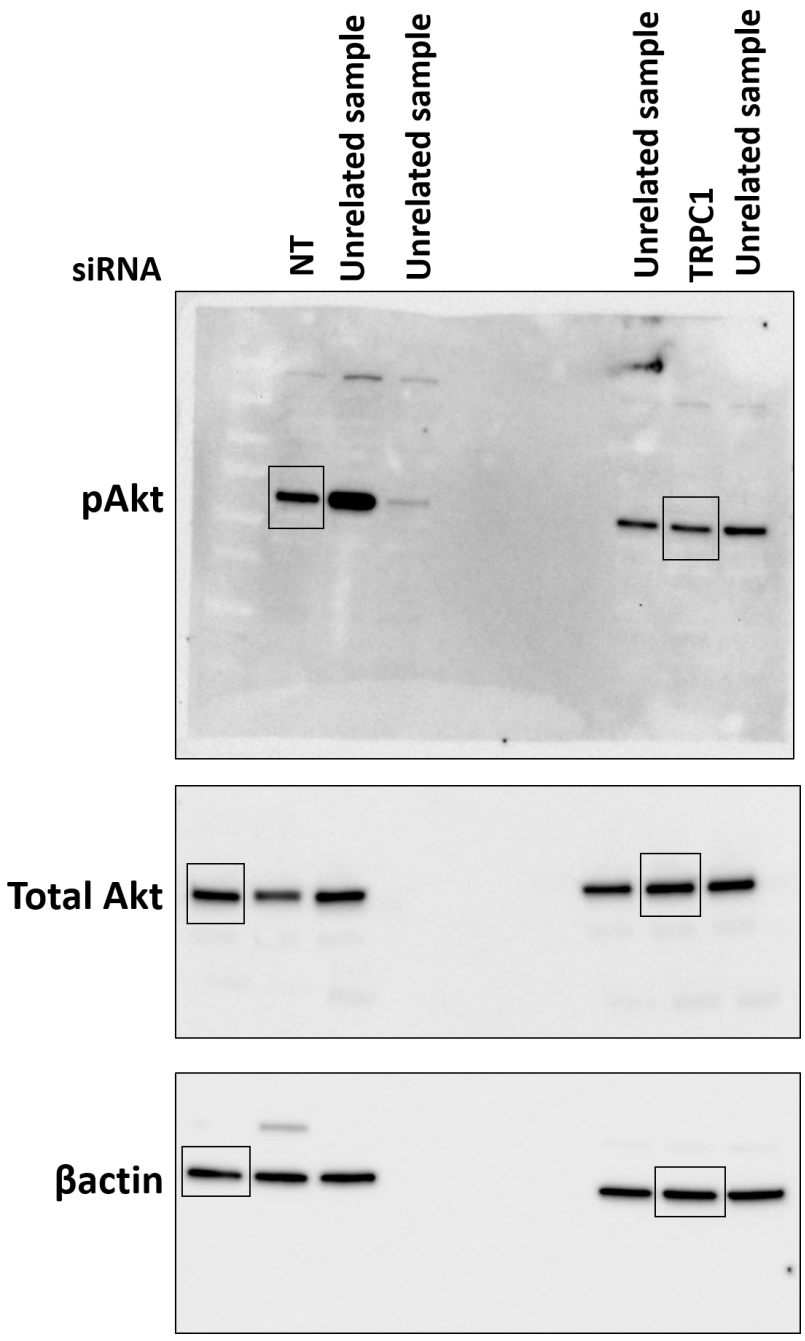

Figure S5. The uncropped images of Fig. 4Gii with indicated areas of selection highlighted in black.

Journal of Cell Science • Supplementary information

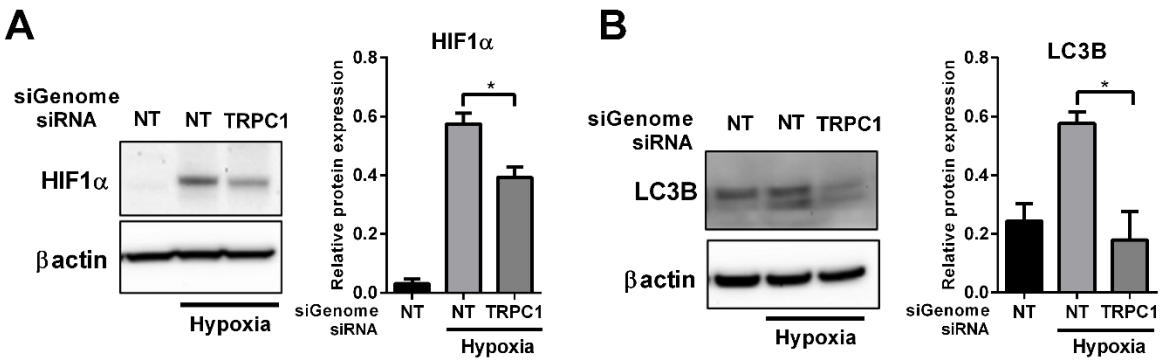

Figure S6. The effects of TRPC1 silencing on the (**A**) HIF1α levels after hypoxia and (**B**) hypoxia-induced LC3B expression were confirmed using a different siRNA chemistry (Dharmacon siGENOME) (n=3, mean ± SD, *$p < 0.001$, Bonferroni one-way ANOVA).

Journal of Cell Science • Supplementary information

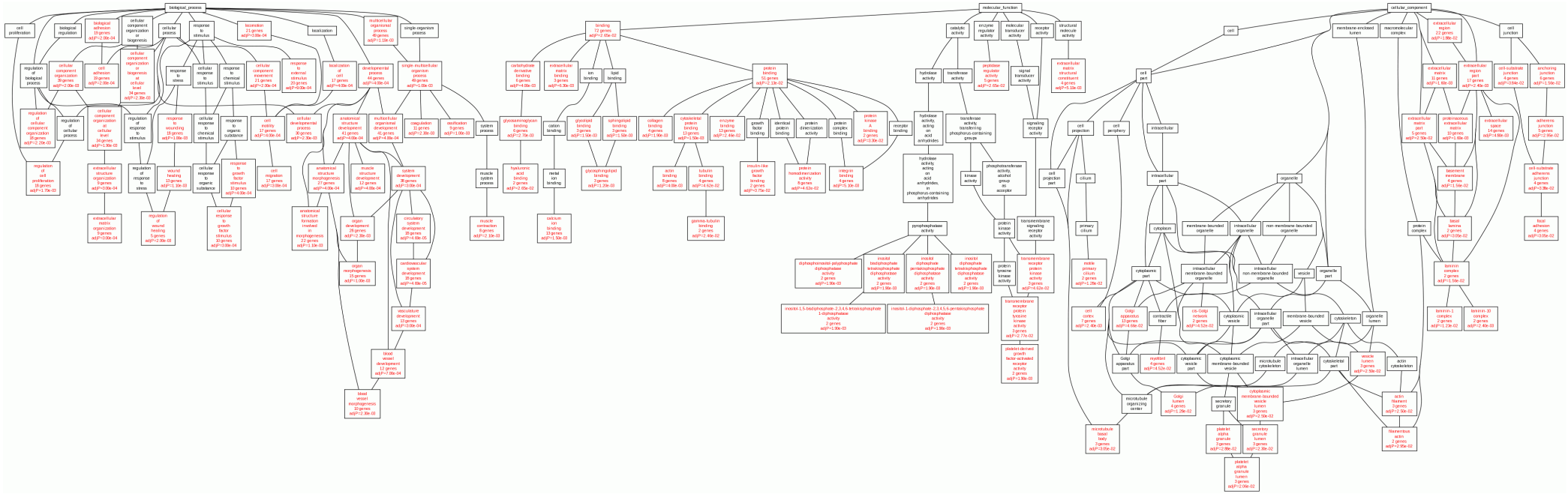
biological_process
cell proliferation
biological regulation
biological adhesion 19 genes adjP=2.00e-04
cellular component organization or biogenesis
cellular process
response to stimulus
locomotion 21 genes adjP=3.00e-04
localization
multicellular organismal process 69 genes adjP=1.10e-03
single-organism process
regulation of biological process
cellular component organization 39 genes adjP=2.00e-03
cell adhesion 19 genes adjP=2.00e-04
cellular component organization or biogenesis at cellular level 34 genes adjP=2.30e-03
response to stimulus
cellular response to stimulus
response to chemical stimulus
cellular component movement 21 genes adjP=2.00e-04
response to external stimulus 20 genes adjP=9.00e-04
localization of cell 17 genes adjP=4.00e-04
developmental process 44 genes adjP=4.00e-04
single-multicellular organism process 48 genes adjP=1.00e-03
regulation of cellular component organization 37 genes adjP=2.20e-03
regulation of cellular process
cellular component organization at cellular level 34 genes adjP=1.30e-03
regulation of response to stimulus
response to wounding 15 genes adjP=1.00e-03
cellular response to chemical stimulus
response to organic substance
cell motility 17 genes adjP=1.60e-04
cellular developmental process 30 genes adjP=2.30e-03
anatomical structure development 41 genes adjP=4.00e-04
multicellular organismal development 41 genes adjP=4.00e-04
coagulation 11 genes adjP=2.30e-03
death 9 genes adjP=1.00e-03
system process
regulation of cellular component organization 37 genes adjP=1.70e-03
extracellular structure organization 5 genes adjP=3.00e-04
regulation of response to stress
wound healing 13 genes adjP=1.30e-03
cellular response to organic substance
response to growth factor stimulus 10 genes adjP=4.00e-04
cell migration 17 genes adjP=3.00e-04
anatomical structure morphogenesis 27 genes adjP=4.00e-04
muscle structure development 12 genes adjP=4.00e-04
system development 36 genes adjP=2.00e-04
muscle system process
extracellular structure organization 5 genes adjP=3.00e-04
regulation of wound healing 5 genes adjP=2.00e-03
anatomical structure formation involved in morphogenesis 22 genes adjP=1.10e-03
organ development 25 genes adjP=2.30e-03
circulatory system development 18 genes adjP=3.60e-05
organ morphogenesis 15 genes adjP=1.00e-03
cardiovascular system development 18 genes adjP=4.60e-05
vasculature development 13 genes adjP=3.00e-04
blood vessel development 10 genes adjP=7.90e-04
blood vessel morphogenesis 10 genes adjP=2.30e-03
muscle contraction 8 genes adjP=2.10e-03
hyaluronic acid binding 2 genes adjP=2.60e-02
glycosaminoglycan binding 6 genes adjP=2.70e-03
carbohydrate derivative binding 6 genes adjP=4.00e-03
extracellular matrix binding 3 genes adjP=1.60e-03
binding 72 genes adjP=2.60e-02
cation binding
ion binding
lipid binding
metal ion binding
calcium ion binding 13 genes adjP=1.50e-03
glycolipid binding 3 genes adjP=1.50e-03
sphingolipid binding 3 genes adjP=1.50e-03
glycosphingolipid binding 2 genes adjP=1.20e-03
collagen binding 4 genes adjP=1.90e-03
protein binding 51 genes adjP=2.10e-02
cytoskeletal protein binding 13 genes adjP=1.50e-03
actin binding 8 genes adjP=4.00e-03
tubulin binding 4 genes adjP=3.62e-02
gamma-tubulin binding 2 genes adjP=2.40e-02
enzyme binding 13 genes adjP=2.40e-02
growth factor binding 2 genes adjP=5.70e-02
identical protein binding
protein dimerization activity
protein complex binding
insulin like growth factor binding 2 genes adjP=5.70e-02
protein homodimerization activity 9 genes adjP=4.62e-02
protein kinase A binding 2 genes adjP=3.30e-02
integrin binding 4 genes adjP=5.30e-03
receptor binding
molecular_function
catalytic activity
enzyme regulator activity
molecular transducer activity
receptor activity
structural molecule activity
hydrolase activity
transferase activity
peptidase regulator activity 5 genes adjP=2.60e-02
signal transducer activity
extracellular matrix structural constituent 4 genes adjP=5.10e-03
hydrolase activity, acting on acid anhydrides
transferase activity, transferring phosphorus-containing groups
signaling receptor activity
receptor binding
hydrolase activity, acting on acid anhydrides, in phosphorus-containing anhydrides
phosphotransferase activity, alcohol group as acceptor
kinase activity
pyrophosphatase activity
protein kinase activity
transmembrane signaling receptor activity
diphosphoinositol-polyphosphate diphosphatase activity 2 genes adjP=1.90e-03
inositol bisphosphate 5-phosphatase activity 2 genes adjP=1.90e-03
inositol diphosphate phosphohydrolase activity 2 genes adjP=1.90e-03
inositol diphosphate tetrakisphosphate diphosphatase activity 2 genes adjP=1.90e-03
protein tyrosine kinase activity
transmembrane receptor protein kinase activity 3 genes adjP=3.62e-03
inositol-4,5-bisdiphosphate-2,3,4,5-tetrakisphosphate 1-diphosphatase activity 2 genes adjP=1.90e-03
inositol-1-diphosphate-2,3,4,5,6-pentakisphosphate diphosphatase activity 2 genes adjP=1.90e-03
transmembrane receptor protein tyrosine kinase activity adjP=2.77e-02
platelet derived growth factor activated receptor activity 2 genes adjP=1.90e-03
cellular_component
cell
membrane-enclosed lumen
macromolecular complex
extracellular region 22 genes adjP=1.80e-02
cell junction
cell part
extracellular matrix 11 genes adjP=1.90e-03
extracellular region part 17 genes adjP=2.40e-03
cell-substrate junction 4 genes adjP=2.80e-02
anchoring junction 5 genes adjP=1.50e-02
extracellular matrix part 5 genes adjP=2.30e-02
proteinaceous extracellular matrix 10 genes adjP=3.00e-03
extracellular space 14 genes adjP=4.90e-03
adherens junction 5 genes adjP=2.90e-02
cell projection part
cilium
primary cilium 2 genes adjP=1.20e-02
motile primary cilium 2 genes adjP=1.20e-02
intracellular part
basement membrane 4 genes adjP=1.50e-03
cell-substrate adherens junction 4 genes adjP=2.30e-02
cytoplasm
membrane-bounded organelle
intracellular organelle
non-membrane-bounded organelle
basal lamina 2 genes adjP=2.00e-02
protein complex
laminin complex 2 genes adjP=1.50e-02
cytoplasmic part
intracellular membrane-bounded organelle
intracellular non-membrane-bounded organelle
vesicle
organelle part
laminin-1 complex 2 genes adjP=1.10e-02
laminin-10 complex 4 genes adjP=2.40e-03
cell cortex 3 genes adjP=2.40e-03
Golgi apparatus 13 genes adjP=8.60e-02
centriolar filter
cis-Golgi network 2 genes adjP=4.52e-02
cytoplasmic vesicle
intracellular organelle part
membrane-bounded vesicle
cytoskeleton
organelle lumen
Golgi apparatus part
myeloid 4 genes adjP=4.52e-02
cytoplasmic vesicle part
cytoplasmic membrane-bounded vesicle
intracellular organelle lumen
cytoskeletal part
vesicle lumen 4 genes adjP=2.50e-02
actin cytoskeleton
microtubule organizing center
Golgi lumen 4 genes adjP=1.20e-02
secretory granule
cytoplasmic membrane-bounded vesicle lumen 3 genes adjP=2.50e-02
actin filament 3 genes adjP=2.50e-02
microtubule basal body 3 genes adjP=3.05e-02
platelet alpha granule 3 genes adjP=2.90e-02
secretory granule lumen 3 genes adjP=2.30e-02
filamentous actin 2 genes adjP=2.30e-02
platelet alpha granule lumen 2 genes adjP=2.00e-02

Figure S7. Gene ontology hierarchical trees for genes positively correlated to *TRPC1* for biological processes, molecular functions and cellular components.

Journal of Cell Science • Supplementary information

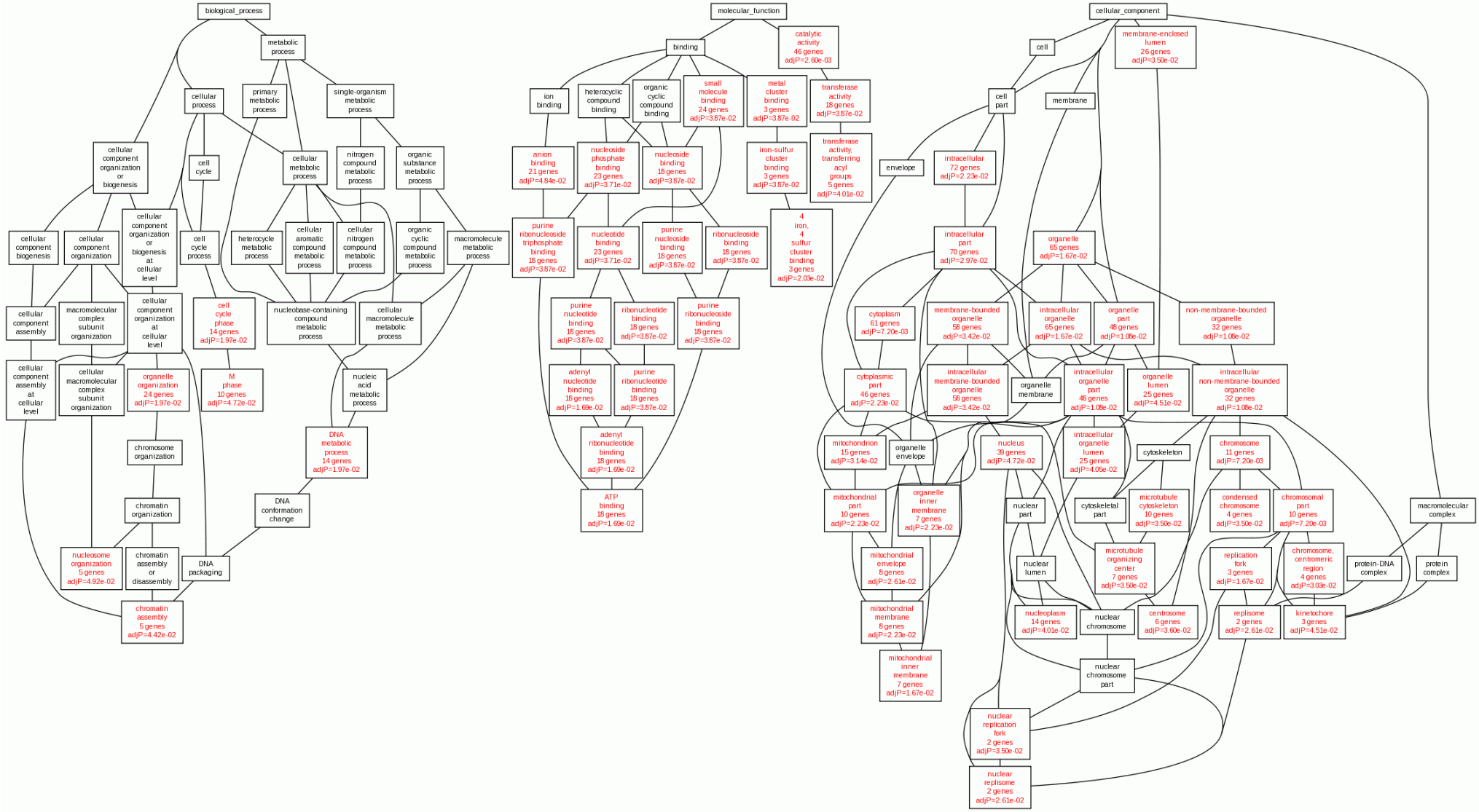
biological_process
metabolic process
cellular process
primary metabolic process
single-organism metabolic process
cellular component organization or biogenesis
cell cycle
cellular metabolic process
nitrogen compound metabolic process
organic substance metabolic process
cellular component biogenesis
cellular component organization
cellular component organization or biogenesis at cellular level
cell cycle process
heterocycle metabolic process
cellular aromatic compound metabolic process
cellular nitrogen compound metabolic process
organic cyclic compound metabolic process
macromolecule metabolic process
cellular component assembly
macromolecular complex subunit organization
cellular component organization at cellular level
cell cycle phase 14 genes adjP=1.97e-02
nucleobase-containing compound metabolic process
cellular macromolecule metabolic process
cellular component assembly at cellular level
cellular macromolecular complex subunit organization
organelle organization 24 genes adjP=1.97e-02
M phase 10 genes adjP=4.72e-02
nucleic acid metabolic process
chromosome organization
DNA metabolic process 14 genes adjP=1.97e-02
chromatin organization
DNA conformation change
nucleosome organization 5 genes adjP=4.92e-02
chromatin assembly or disassembly
DNA packaging
chromatin assembly 5 genes adjP=4.42e-02
molecular_function
binding
catalytic activity 46 genes adjP=2.60e-03
ion binding
heterocyclic compound binding
organic cyclic compound binding
small molecule binding 24 genes adjP=3.87e-02
metal cluster binding 3 genes adjP=3.87e-02
transferase activity 18 genes adjP=3.87e-02
anion binding 21 genes adjP=4.84e-02
nucleoside phosphate binding 23 genes adjP=3.71e-02
nucleoside binding 18 genes adjP=3.87e-02
iron-sulfur cluster binding 3 genes adjP=3.87e-02
transferase activity, transferring acyl groups 5 genes adjP=4.01e-02
purine ribonucleoside triphosphate binding 16 genes adjP=3.87e-02
nucleotide binding 23 genes adjP=3.71e-02
purine nucleoside binding 18 genes adjP=3.87e-02
ribonucleoside binding 18 genes adjP=3.87e-02
4 iron, 4 sulfur cluster binding 3 genes adjP=2.03e-02
purine nucleotide binding 18 genes adjP=3.87e-02
ribonucleotide binding 18 genes adjP=3.87e-02
purine ribonucleoside binding 18 genes adjP=3.87e-02
adenyl nucleotide binding 18 genes adjP=1.69e-02
purine ribonucleotide binding 18 genes adjP=3.87e-02
adenyl ribonucleotide binding 18 genes adjP=1.69e-02
ATP binding 18 genes adjP=1.69e-02
cellular_component
cell
membrane-enclosed lumen 26 genes adjP=3.50e-02
cell part
membrane
envelope
intracellular 72 genes adjP=2.23e-02
intracellular part 70 genes adjP=2.97e-02
organelle 65 genes adjP=1.67e-02
cytoplasm 61 genes adjP=7.20e-03
membrane-bounded organelle 58 genes adjP=3.42e-02
intracellular organelle 65 genes adjP=1.67e-02
organelle part 48 genes adjP=1.08e-02
non-membrane-bounded organelle 32 genes adjP=1.08e-02
cytoplasmic part 46 genes adjP=2.23e-02
intracellular membrane-bounded organelle 58 genes adjP=3.42e-02
organelle membrane
intracellular organelle part 48 genes adjP=1.08e-02
organelle lumen 25 genes adjP=4.51e-02
intracellular non-membrane-bounded organelle 32 genes adjP=1.06e-02
mitochondrion 15 genes adjP=3.14e-02
organelle envelope
nucleus 39 genes adjP=4.72e-02
intracellular organelle lumen 25 genes adjP=4.05e-02
cytoskeleton
chromosome 11 genes adjP=7.20e-03
mitochondrial part 10 genes adjP=2.23e-02
organelle inner membrane 7 genes adjP=2.23e-02
nuclear part
cytoskeletal part
microtubule cytoskeleton 10 genes adjP=3.50e-02
condensed chromosome 4 genes adjP=3.50e-02
chromosomal part 10 genes adjP=7.20e-03
macromolecular complex
mitochondrial envelope 8 genes adjP=2.61e-02
nuclear lumen
microtubule organizing center 7 genes adjP=3.50e-02
replication fork 3 genes adjP=1.67e-02
chromosome, centromeric region 4 genes adjP=3.03e-02
protein-DNA complex
protein complex
mitochondrial membrane 8 genes adjP=2.23e-02
nucleoplasm 14 genes adjP=4.01e-02
nuclear chromosome
centrosome 6 genes adjP=3.60e-02
replisome 2 genes adjP=2.61e-02
kinetochore 3 genes adjP=4.51e-02
mitochondrial inner membrane 7 genes adjP=1.67e-02
nuclear chromosome part
nuclear replication fork 2 genes adjP=3.50e-02
nuclear replisome 2 genes adjP=2.61e-02

Figure S8. Gene ontology hierarchical trees for genes negatively correlated to *TRPC1* for biological processes, molecular functions and cellular components.

Journal of Cell Science • Supplementary information

Table S1. List of the top 50 positively correlated genes with *TRPC1* expression.

	Gene Symbol	Pearson Score	Spearman Score		Gene Symbol	Pearson Score	Spearman Score
1	NAP1L3	0.63	0.63	51	CEP112	0.5	0.5
2	MARVELD1	0.62	0.59	52	FERMT2	0.5	0.5
3	JAM3	0.59	0.61	53	MAGEL2	0.5	0.5
4	MSRB3	0.58	0.61	54	HABP4	0.5	0.5
5	RECK	0.58	0.59	55	CLIP3	0.5	0.5
6	PLS3	0.58	0.56	56	ISM1	0.5	0.49
7	MICU3	0.57	0.59	57	TSPAN2	0.5	0.48
8	STARD9	0.57	0.58	58	DGKI	0.49	0.53
9	PKD2	0.57	0.54	59	CALD1	0.49	0.52
10	TPST1	0.57	0.54	60	DCN	0.49	0.52
11	PRKD1	0.55	0.6	61	BACH2	0.49	0.51
12	LRCH2	0.55	0.56	62	YPEL4	0.49	0.51
13	DDR2	0.55	0.55	63	PROS1	0.49	0.5
14	IL17D	0.55	0.55	64	AKAP12	0.49	0.5
15	ZNF521	0.55	0.55	65	COPZ2	0.49	0.5
16	MYLK	0.54	0.56	66	DKK3	0.49	0.5
17	BACE1	0.54	0.56	67	CYP2U1	0.49	0.48
18	GAS1	0.54	0.55	68	TBX18	0.48	0.52
19	NPR2	0.54	0.55	69	TMEM204	0.48	0.5
20	LAYN	0.54	0.55	70	CNN1	0.48	0.49
21	DACT3	0.54	0.55	71	SPARC	0.48	0.49
22	FLRT2	0.54	0.53	72	CCDC8	0.48	0.49
23	LARP6	0.54	0.52	73	PDGFRA	0.48	0.48
24	LAMB1	0.53	0.56	74	PTRF	0.47	0.51
25	SNAI2	0.53	0.55	75	PDGFRL	0.47	0.5
26	CNRIP1	0.53	0.55	76	CDH11	0.47	0.49
27	ULK4P1	0.53	0.53	77	VCAN	0.47	0.49
28	KDELC1	0.53	0.52	78	BEND6	0.47	0.49
29	GAS6	0.52	0.55	79	FAP	0.47	0.48
30	FSTL1	0.52	0.55	80	TPM2	0.47	0.48
31	FEZ1	0.52	0.54	81	LHFP	0.47	0.48
32	LIMS2	0.52	0.54	82	DZIP1	0.46	0.52
33	GPR124	0.52	0.54	83	RCBTB2	0.46	0.51
34	SRPX	0.52	0.53	84	HSPB2	0.46	0.49
35	PCDH18	0.52	0.53	85	TAGLN	0.46	0.49
36	PPAPDC3	0.52	0.53	86	HAND2	0.46	0.49
37	STON1	0.52	0.51	87	FHL1	0.46	0.48
38	NDN	0.51	0.56	88	ETV1	0.46	0.48
39	GLT8D2	0.51	0.54	89	FOXO1	0.46	0.48
40	ECM2	0.51	0.53	90	C14ORF37	0.46	0.48
41	ZFPM2	0.51	0.53	91	PLSCR4	0.45	0.49
42	TSHZ3	0.51	0.53	92	CAV1	0.45	0.48
43	GLI2	0.51	0.52	93	FBLN1	0.45	0.48
44	VIM	0.51	0.52	94	NUDT10	0.44	0.51
45	LAMC1	0.51	0.5	95	C1S	0.44	0.48
46	NUDT11	0.5	0.56	96	FBLN2	0.44	0.48
47	RBMS3	0.5	0.53	97	DAAM2	0.43	0.49
48	IGFBP7	0.5	0.52	98	RNF150	0.43	0.49
49	SYNE1	0.5	0.51	99	EVC2	0.42	0.48
50	CTGF	0.5	0.5	100	PRTFDC1	0.41	0.5

Journal of Cell Science • Supplementary information

Table S2. List of the top 50 negatively correlated genes with *TRPC1* expression.

	Gene Symbol	Pearson Score	Spearman Score		Gene Symbol	Pearson Score	Spearman Score
1	SLC25A10	-0.41	-0.42	51	CASC5	-0.3	-0.33
2	RNF151	-0.41	-0.41	52	NSUN5	-0.31	-0.33
3	C16ORF13	-0.4	-0.41	53	POC1A	-0.32	-0.33
4	FAM195A	-0.39	-0.4	54	DCST2	-0.32	-0.33
5	PROSER3	-0.39	-0.4	55	FLVCR1	-0.31	-0.33
6	TOR2A	-0.39	-0.4	56	ACVR1B	-0.31	-0.32
7	IDE	-0.37	-0.39	57	CPT2	-0.35	-0.32
8	RAD9A	-0.35	-0.39	58	SLC6A18	-0.31	-0.32
9	TAF6L	-0.37	-0.39	59	LRRC45	-0.32	-0.32
10	DHTKD1	-0.37	-0.39	60	CENPM	-0.3	-0.32
11	MRPS34	-0.39	-0.38	61	FLAD1	-0.32	-0.32
12	SMPD2	-0.37	-0.38	62	TARS2	-0.32	-0.32
13	BDH1	-0.37	-0.36	63	ASF1B	-0.29	-0.32
14	LBHD1	-0.32	-0.36	64	POLA2	-0.31	-0.32
15	C16ORF59	-0.33	-0.36	65	MIS18A	-0.31	-0.32
16	PSENEN	-0.35	-0.36	66	RHBDD3	-0.3	-0.32
17	ZNHIT2	-0.34	-0.35	67	NMRAL1	-0.31	-0.32
18	BRI3BP	-0.34	-0.35	68	NADK	-0.31	-0.32
19	HMGA1	-0.34	-0.35	69	XPNPEP3	-0.32	-0.32
20	NDUFS8	-0.3	-0.35	70	PAQR4	-0.34	-0.32
21	TONSL	-0.35	-0.35	71	SOCS7	-0.24	-0.32
22	PKMYT1	-0.34	-0.35	72	IFNL2	-0.27	-0.31
23	SAC3D1	-0.34	-0.35	73	DAB1	-0.29	-0.31
24	NARFL	-0.36	-0.35	74	KIR3DL1	-0.27	-0.31
25	H2AFX	-0.32	-0.34	75	NFKBIB	-0.3	-0.31
26	MAP3K9	-0.33	-0.34	76	RPUSD1	-0.3	-0.31
27	ATP8B1	-0.35	-0.34	77	NACC1	-0.29	-0.31
28	RREB1	-0.34	-0.34	78	AIFM1	-0.31	-0.31
29	ALG3	-0.31	-0.34	79	PIP5K1A	-0.33	-0.31
30	EHMT2	-0.32	-0.34	80	FAM20B	-0.31	-0.31
31	CEP250	-0.31	-0.34	81	DPP3	-0.33	-0.31
32	PAK4	-0.34	-0.34	82	ESPL1	-0.27	-0.31
33	SLC50A1	-0.34	-0.34	83	DHX34	-0.32	-0.31
34	SPIRE2	-0.33	-0.34	84	TIMM17B	-0.29	-0.31
35	ARHGEF39	-0.32	-0.34	85	TBL3	-0.31	-0.31
36	TJP3	-0.3	-0.34	86	COPE	-0.28	-0.31
37	CHTF18	-0.31	-0.34	87	MTFP1	-0.32	-0.31
38	CKS2	-0.31	-0.33	88	PPME1	-0.29	-0.31
39	KIF22	-0.33	-0.33	89	EMC9	-0.31	-0.31
40	PRDX2	-0.31	-0.33	90	CDC42BPG	-0.3	-0.31
41	XRCC3	-0.32	-0.33	91	C7ORF43	-0.32	-0.31
42	ADAM15	-0.34	-0.33	92	ZNF587	-0.3	-0.31
43	UBAP2L	-0.33	-0.33	93	ZDHHC12	-0.32	-0.31
44	NUBP2	-0.33	-0.33	94	FBXL6	-0.31	-0.31
45	NAA40	-0.32	-0.33	95	DAZAP1	-0.28	-0.31
46	CDK2AP2	-0.32	-0.33	96	BRMS1	-0.3	-0.31
47	LCE3B	-0.3	-0.33	97	FAM111B	-0.27	-0.31
48	SRRT	-0.31	-0.33	98	KLC2	-0.29	-0.31
49	MXD3	-0.29	-0.33	99	MRPS26	-0.28	-0.31
50	AGPAT3	-0.32	-0.33	100	DUS1L	-0.31	-0.31

Journal of Cell Science • Supplementary information